

Eastern Kentucky University

Encompass

---

Honors Theses

Student Scholarship

---

Fall 11-30-2020

## Making and Characterizing Semiconducting Polymer for Organic Electronics

Jessica Bone

[jessica\\_bone1@mymail.eku.edu](mailto:jessica_bone1@mymail.eku.edu)

Follow this and additional works at: [https://encompass.eku.edu/honors\\_theses](https://encompass.eku.edu/honors_theses)

---

### Recommended Citation

Bone, Jessica, "Making and Characterizing Semiconducting Polymer for Organic Electronics" (2020). *Honors Theses*. 781.

[https://encompass.eku.edu/honors\\_theses/781](https://encompass.eku.edu/honors_theses/781)

This Open Access Dissertation is brought to you for free and open access by the Student Scholarship at Encompass. It has been accepted for inclusion in Honors Theses by an authorized administrator of Encompass. For more information, please contact [Linda.Sizemore@eku.edu](mailto:Linda.Sizemore@eku.edu).

# Eastern Kentucky University

Making and Characterizing Semiconducting Polymer for Organic Electronics

Honors Thesis  
Submitted  
In Partial Fulfillment  
of the  
Requirements of HON 420  
Fall 2020

By  
Jessica Bone

Mentor  
Dr. Judith L. Jenkins  
Department of Chemistry

# Making and Characterizing Semiconducting Polymer for Organic Electronics

Jessica Bone

Dr. Judith L. Jenkins  
Department of Chemistry

## **Abstract**

Advances in organic electronics are limited by the need for materials that effectively conduct both electrons and ions while also meeting other design criteria (cheap, flexible, stable, etc.) Conducting polymers are exciting candidates for platforms requiring mixed ionic-electronic conduction as they have a wide range of possibilities due to the ability to synthetically control the monomer unit. However, it is difficult to predict how the monomer properties influence the polymer film properties. In order to make functional materials, we need to better understand how the properties of the monomer (size, shape, functional groups, frontier orbital energies) will influence the resulting polymer. In this work we describe the electropolymerization and electrodeposition of poly(3-dodecylthiophene) (P3DDT), building on similar examinations of poly(3-hexylthiophene). We show that P3DDT can be electropolymerized and electrodeposited onto an ITO substrate. Correlations between the charge passed during electrodeposition and the resulting film properties (amount of electroactive polymer and polymer film morphology) are discussed. The information gained from this work provides information necessary for the design of future functional materials.

**Keywords:** semiconducting polymer, organic electronic, polymerization, electrodeposition, thiophene

## Table of Contents

<b>List of Figures</b> .....	<b>iv</b>
<b>List of Tables</b> .....	<b>v</b>
<b>Chapter 1: Background and Scope</b> .....	<b>1</b>
1.1 Polymer basics.....	1
1.2 Electronic Properties.....	8
1.3 Applications of Conducting Polymers.....	12
1.4 Polymerization.....	21
1.5 Electropolymerization and Polymer Electrodeposition.....	23
1.6 Electrochemically Stimulated Conformational Relaxation.....	26
1.7 Overview.....	29
<b>Chapter 2: Experimental Methods</b> .....	<b>31</b>
2.1 Materials and Instrumentation.....	31
2.2 Substrate Preparation and Functionalization.....	31
2.3 Electrochemistry.....	32
2.4 Scanning Probe Microscopy.....	34
<b>Chapter 3: Electrochemical polymerization, electrodeposition, and characterization of poly(3-dodecylthiophene) (P3DDT) thin films</b> .....	<b>36</b>
3.1 P3DDT Film Electropolymerization and Deposition.....	36
3.2 P3DDT Film Electronic Properties.....	38
3.3 P3DDT Film Atomic Force Microscopy.....	48
<b>Chapter 4: Future Direction</b> .....	<b>52</b>
<b>References</b> .....	<b>53</b>

## List of Figures

<b>Figure 1.1:</b> Representation of monomers, oligomers, polymer microstructure.....	1
<b>Figure 1.2:</b> Molecular description of noncovalent interactions.....	3
<b>Figure 1.3:</b> Molecular depiction of HDPE and LDPE.....	5
<b>Figure 1.4:</b> Monomer units of common semiconducting polymer.....	7
<b>Figure 1.5:</b> Energy diagram of increasing number of atoms.....	9
<b>Figure 1.6:</b> Energy diagram of conductors, semiconductors, and insulators.....	10
<b>Figure 1.7:</b> Oxidation of thiophene monomer.....	12
<b>Figure 1.8:</b> Depiction of polypyrrole coated electrode.....	13
<b>Figure 1.9:</b> Reaction of polymer-based, lactate biosensor.....	14
<b>Figure 1.10:</b> Depiction of a polymer-based actuator.....	16
<b>Figure 1.11:</b> Structural outline of organic light emitting diode.....	18
<b>Figure 1.12:</b> Structural outline of photovoltaic cell.....	20
<b>Figure 1.13:</b> Two polymerization techniques reaction.....	22
<b>Figure 1.14:</b> Electrochemical synthesis of polythiophene polymer.....	24
<b>Figure 1.15:</b> Electrochemically stimulated conformational relaxation model (ESCR)....	27
<b>Figure 1.16:</b> Structural outline of three thiophene derivatives.....	29
<b>Figure 2.1:</b> Electrodeposition of 3-DDT onto a functionalized ITO electrode.....	33
<b>Figure 2.2:</b> Atomic force microscope (AFM) diagram.....	35
<b>Figure 3.1:</b> Potential step growth of a representative P3DDT film.....	37
<b>Figure 3.2:</b> Relationship of charge to $i_p$ , $E_{1/2}$ , and the integrated charge.....	40
<b>Figure 3.3:</b> Illustrated cyclic voltammogram of P3DDT film.....	43
<b>Figure 3.4:</b> Electrodeposition and cyclic voltammograms of film 1, film 2, and film 3.....	45

<b>Film 3.5:</b> AFM images of film 6, film 2, and film 3.....	48
--	----

### **List of Tables**

<b>Table 3.1:</b> P3DDT Film Characteristics.....	39
---	----

<b>Table 3.2:</b> P3DDT AFM Characteristics.....	50
--	----

## Chapter 1: Background & Scope

### 1.1 Polymer Basics

A polymer is a large molecule consisting of repeating units, referred to as monomers, held together by covalent bonds as shown in Figure 1a. Monomers may be individual atoms, small molecules, or larger macromolecular species. Two monomers bound to one another are referred to as a dimer, three monomers constitute a trimer, and multiple monomers bound together constitute an oligomer.<sup>1</sup> Oligomers bound together form the polymer. Oligomers can bond together in many different ways.

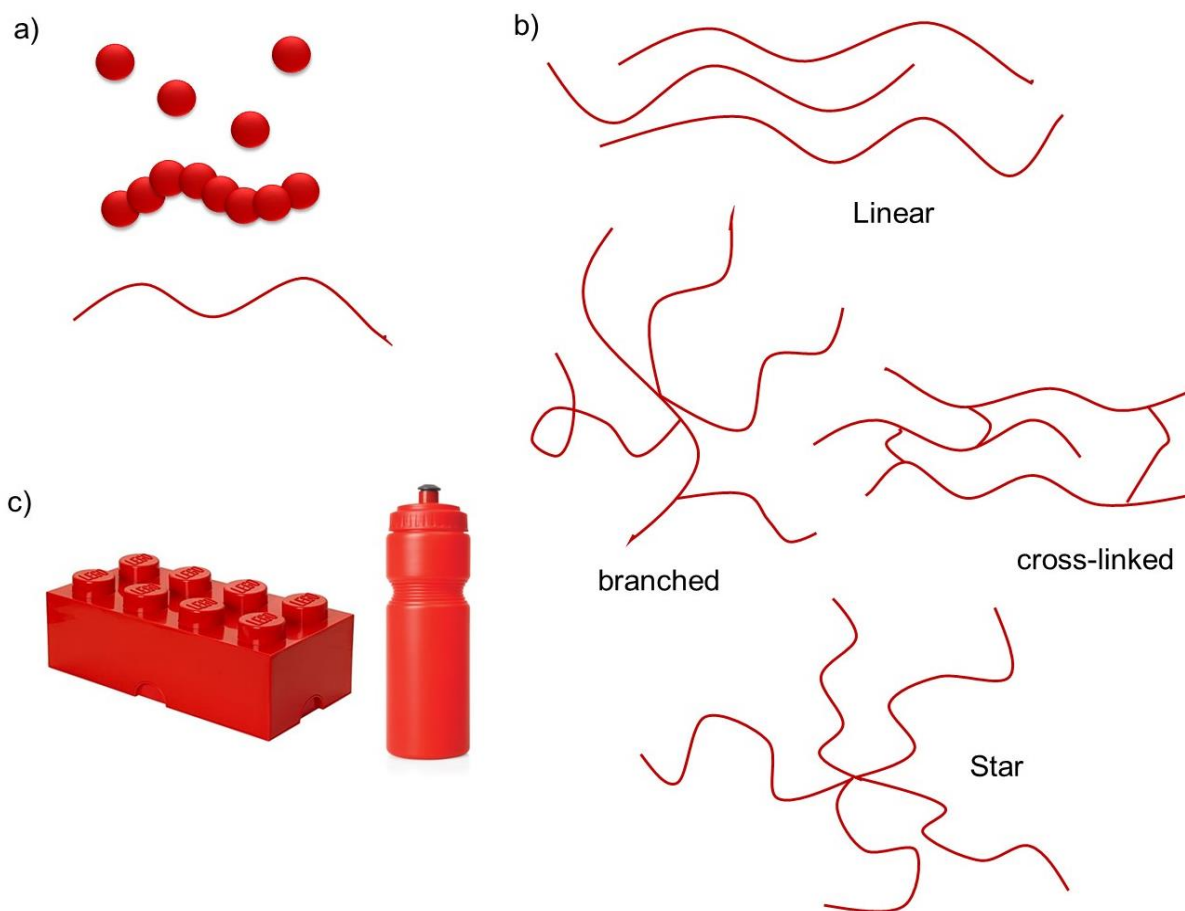


**Figure 1.1.** Cartoon representation of a monomer (one red ball) and an oligomer (multiple red balls) (a). For convenience, polymer fragments are depicted as curvy lines, where each line can represent hundreds or even thousands of monomeric units. Some representative polymer microstructures that arise from differences in the extent of polymer chain branching (b). Everyday products made from polymers (c).

For instance, polymerization can lead to a single chain of oligomers, but polymers can also consist of a primary polymer chain with oligomeric branches. The branches can interact with one another covalently or non-covalently as shown in Figure 1b. Ultimately, the polymers used in daily life consist of multiple millions of the polymer pieces depicted to yield products like the plastic water bottle and the Lego shown in Figure 1c.<sup>2</sup>

Chain length differences make it difficult to measure the molecular weight of a polymer. Figure 1b illustrates several polymer branching styles that can lead to different numbers of polymer chains consisting of different numbers of monomers. To provide a more accurate description of the polymer, an average molecular weight is obtained, where the molecular weight of each chain is determined, and then the molecular weight is averaged per monomer unit.<sup>3</sup> The average molecular weight provides information about the weight distribution of the polymer whereas the molecular weight only describes how much the polymer weighs.<sup>2,3</sup>

Several factors contribute to polymer properties. Specifically, the chain length, the extent of chain branching, and the chemical identity of the monomer all influence the properties and therefore the functions of the resulting polymers.<sup>1,4</sup> In addition to the covalent carbon-carbon and carbon-hydrogen bonds, these polymer chains interact non-covalently through dispersion forces, shown in Figure 1.2. Non-covalent interactions can induce order (also referred to as crystallinity) amongst polymer chains, further influencing the properties of the polymer.<sup>4</sup>



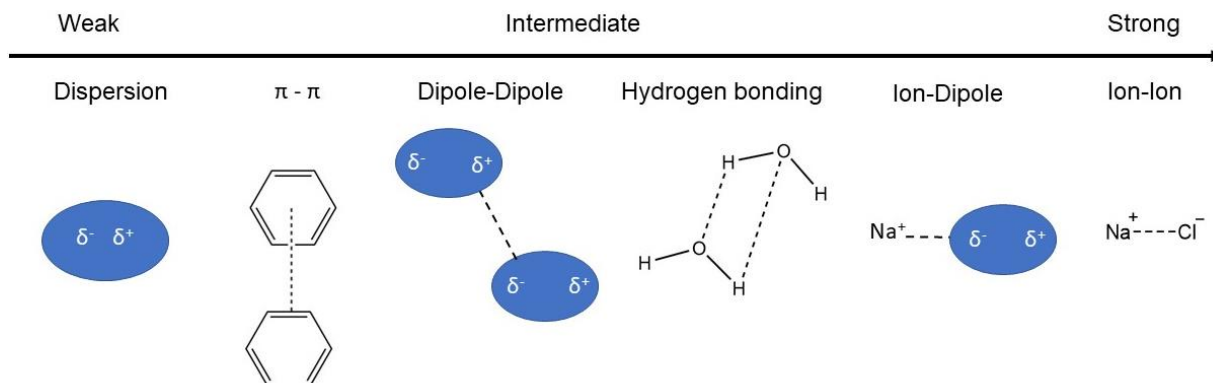


**Figure 1.2.** A molecular description of the noncovalent interactions that can be experienced by a molecule as a function of interaction strength. The weakest interactions are dispersion forces, which arise from interactions between temporary dipoles in two or more species. Pi-pi ( $\pi$ - $\pi$ ) interactions are a specific type of dispersion forces common to species with conjugated pi systems. These interactions occur between an electron deficient ring center, and the electron dense  $\pi$ -bonds in another molecule. Dipole-dipole interactions occur between two or more molecules that have permanent net dipoles. Hydrogen bonding is a specific type of dipole-dipole interaction that occurs between a partially positive hydrogen and a partially negative N, O, or F bound to a hydrogen. An ion-dipole interaction occurs between an ion and a molecule with a permanent net dipole. Ion-Ion interactions occur between two charged species.

Polyethylene, which can exist in both high density and low density configurations, demonstrates the extent to which differences in polymer branching and noncovalent interactions influence polymer properties as shown in Figure 1.3.<sup>5</sup> High-density polyethylene (HDPE) is typically composed of very long polymer chains that are highly branched. As a result, HDPE is very compact and rigid and experiences a high degree of crystallinity. Low density polyethylene experiences less branching, and in turn is less dense, compact, and rigid.<sup>3</sup> Noncovalent interactions do occur in LDPE, but these noncovalent interactions can be overcome by adding only small amounts of energy in the form of physical pushes and pulls. The extensive network of noncovalent interactions throughout the HDPE require substantially more energy to disrupt. A common product

made of HDPE is plastic pipes. These pipes are very strong and not flexible because of the rigidity and high degree of crystallinity occurring at the molecular level in the polymer. Thin plastic bags are often made of LDPE. These bags are very thin, highly flexible, and can stretch with tension. These features are also a reflection of the polymer structure at the molecular, where there is much less rigidity and crystallization.

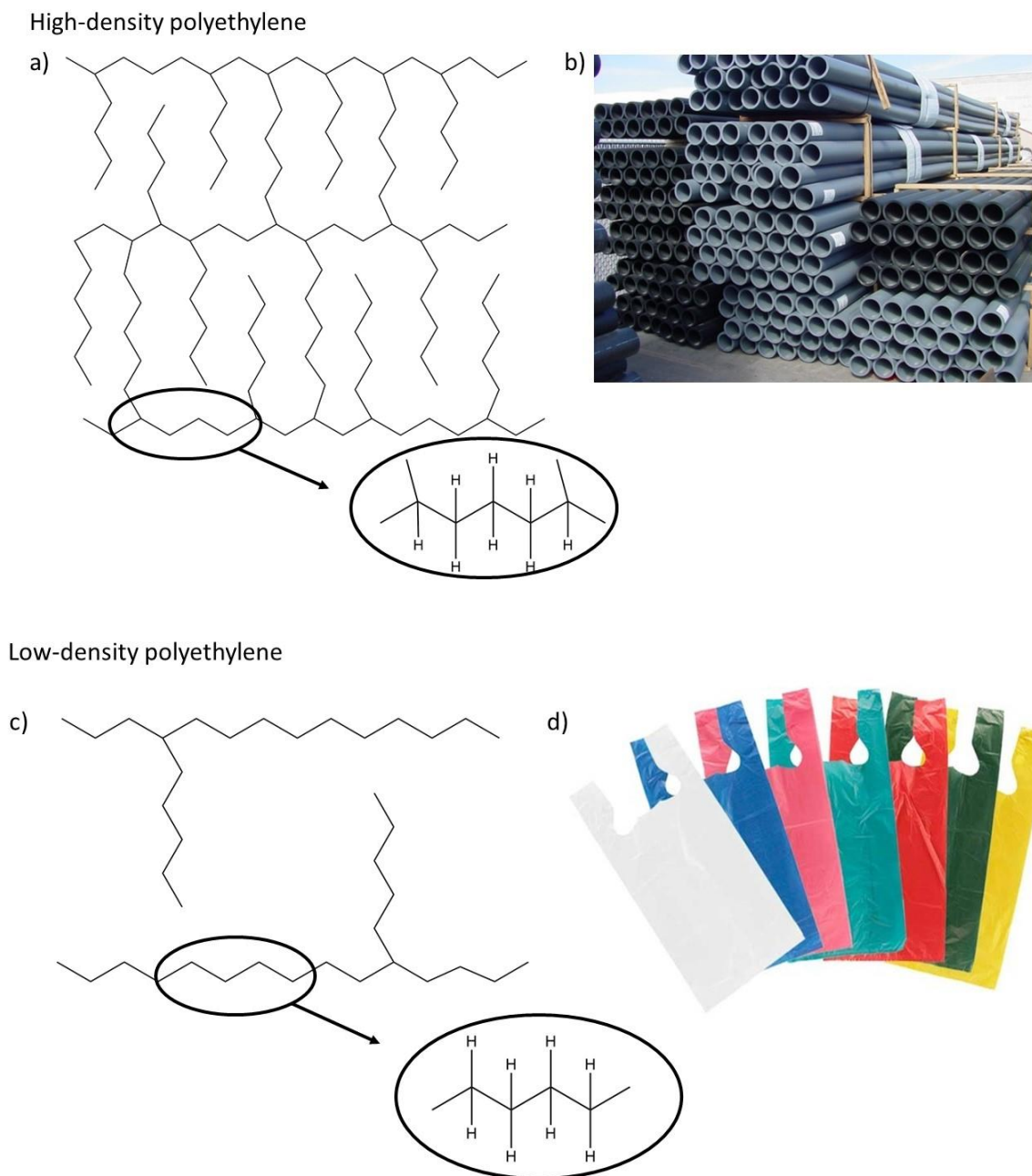


**Figure 1.3.** A molecular level depiction of the high-density polyethylene (a, HDPE), which exhibits highly branched, close-packed polymer chains and is used to make rigid materials such as pipes (b). A molecular level depiction of low-density polyethylene (c, LDPE), which exhibits less branching and loosely packed polymer chains and is used to make thin, flexible materials such as plastic bags.

Chain length and crosslinking also influence properties of the polymer. Crosslinking occurs when chains connect to each other. In Figure 1.1b the crosslinked polymer has chains connecting the two main chains. Crosslinking keeps the longer chains from rearranging when stretched. A polymer with very long chains, but little crosslinking, will have a larger degree of chain entanglement.<sup>3</sup> Physically, the polymer will have restricted movement as the long chains tangle into themselves and cannot slide past each other. This type of chain entanglement is another reason that HDPE is so rigid, while the less-tangled LDPE can be stretched.

The chemical composition of the monomer unit also influences the properties of the polymer. Figure 1.4 shows the chemical structures of some common monomers found in conducting polymers. Some monomers, like propylene or polyacetylene, are composed of only carbon and hydrogen, so the noncovalent interactions in these polymers range from relatively weak dispersion forces to pi-pi interactions. Other polymers, like polythiophene or nylon, contain highly electronegative functional groups and single atoms and therefore experience stronger intermolecular forces such as dipole-dipole interactions and hydrogen bonding. The intermolecular forces impact the degradability, strength, and crystallinity of the polymer. For instance, medical grade sutures are often made from a specific polymer with the function of the suture in mind.<sup>6</sup> A suture made from polypropylene experiences only dispersion forces within the structure and is therefore very flexible. The polypropylene sutures are not absorbable into the body because they lack polar functional groups.<sup>7</sup> As a result, polypropylene sutures are not ideal for internal suturing but are useful for external suturing of the skin.<sup>7</sup> Nylon is another example of a

nonabsorbable suture.<sup>7</sup> A suture made from polyglycolide (PGA) experiences dispersion forces, dipole-dipole interactions, and hydrogen bonding forces. A PGA suture has greater tensile strength because it experiences more noncovalent interactions.<sup>7</sup> Additionally, PGA sutures are biodegradable because they can be broken down by the environment inside the body, and so are used to suture internally since they will eventually degrade and not need removal.<sup>7</sup> Enzymes in the body are primarily responsible for the degradation of absorbable sutures.<sup>7</sup>

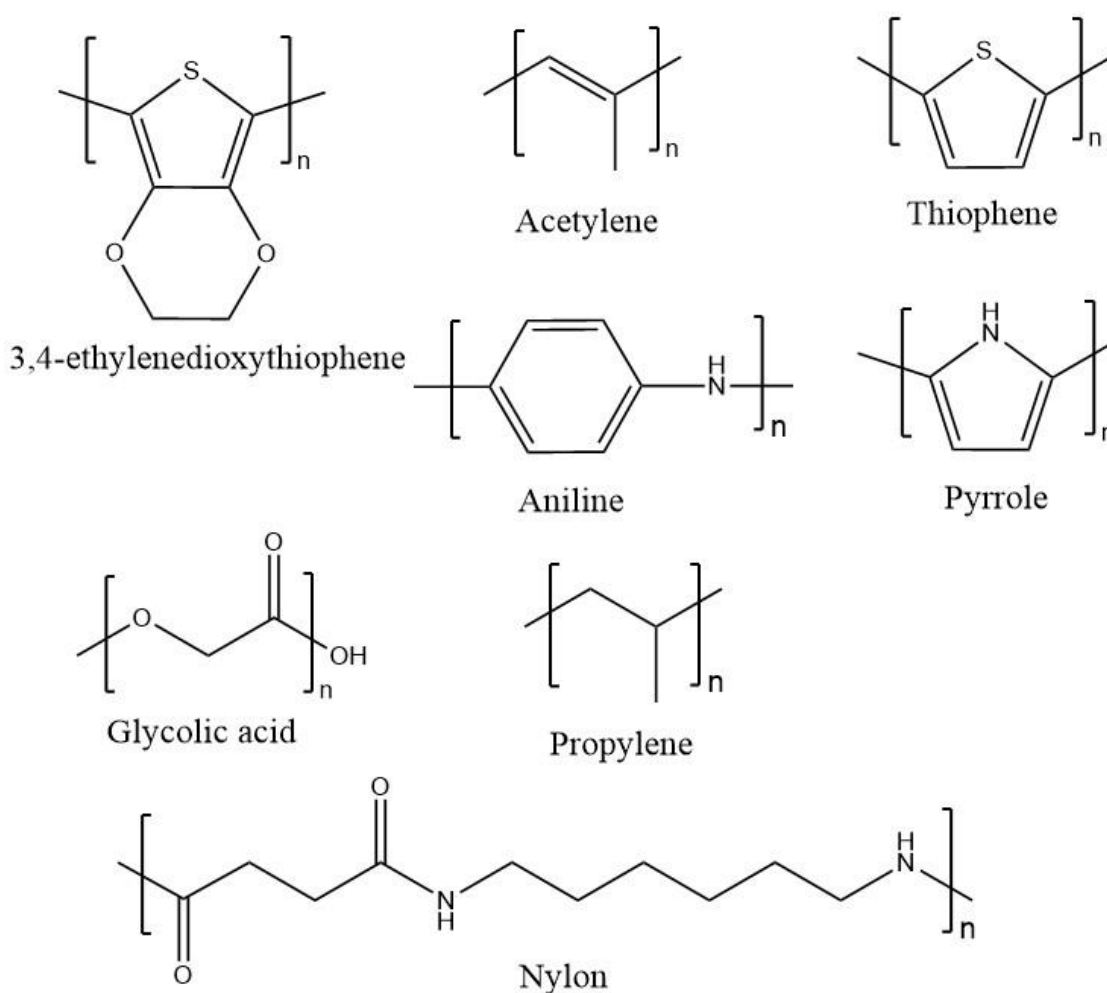


**Figure 1.4.** Structures showing the monomeric units of common conducting polymers.

Though there are a multitude of other interesting polymer properties, the remainder of this introduction will focus on polymers with tunable electronic properties, as the polymer system explored in this work is of interest specifically because of its electronic properties.

## 1.2 Electronic Polymers

Polymers with a  $\pi$ -conjugated system have the ability to conduct electricity.<sup>1,8</sup> A pi ( $\pi$ ) bond is a bond in which there is electron density above and below the internuclear axis as shown in Figure 1.5.<sup>9</sup> A  $\pi$ -conjugated system includes pi-bonds between many consecutive atoms. Because of these pi bonds, electrons can be delocalized across multiple atomic nuclei, or even across multiple monomer units.<sup>9</sup>

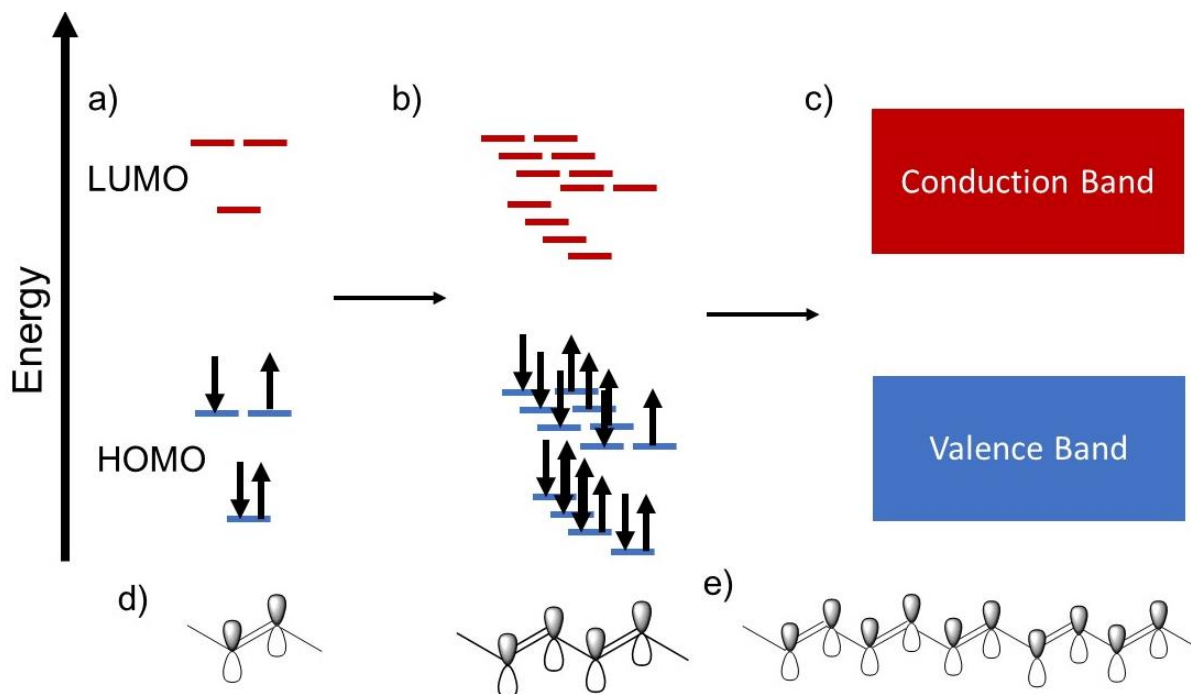


**Figure 1.5.** Energy diagrams as a function of the number of atoms in a system with a focus on the increasing number of p-orbitals as carbon pi-bonds form. The highest occupied molecular orbital (HOMO) is the highest-energy electronic state occupied by an electron. The lowest occupied molecular orbital (LUMO) is the lowest energy electronic state that is not occupied by an electron. As the number of atoms in a pi-system increases, the number of states near the energies of the HOMO and LUMO increase in (a,b). Eventually the number of electronic states becomes so great that they are no longer energetically distinguishable from one another and more easily represented as the valence band (blue, occupied by electrons) and the conduction band (red, unoccupied) (c).

More specifically, the electron delocalization occurs in the  $p_z$  and  $p_y$  orbitals of the carbon backbone.<sup>8,10</sup> The  $p_x$  orbital allows the carbons to form  $\sigma$ -bonds that keep the structure intact and are so low in energy that they are not shown in this diagram.<sup>8</sup> Two carbons are needed to form a bond, and each carbon bring a  $p_z$ ,  $p_x$ , and a  $p_y$  orbital, six orbitals total.<sup>8,10</sup> One of each p-orbital will be involved in the highest occupied molecular orbitals (HOMO), where unexcited electrons are occupying the orbitals at lower energies.<sup>9</sup> One of each p-orbital will be used in the lowest unoccupied molecular orbital (LUMO).<sup>9</sup> These

orbitals are at a higher energy level. Ground state electrons can be excited to these energy levels. As more pi-bonds are formed, and the electronic structure grows as represented by the increasing number of electronic states (red and blue lines in Fig 1.5b). As the number of states increases (corresponding to an increased number of atoms), the states are no longer energetically distinguishable and more easily represented as bands - a valence band and a conduction band (Fig 1.5c).<sup>9</sup> The valence band is occupied by electrons. The conduction band is where electrons are excited to.<sup>9</sup> The conduction band contain orbitals that are unoccupied and lowest in energy.<sup>9</sup>

The relatively small energy gap between the valence band and conduction band is the reason a polymer like this is considered a semiconductor. Figure 1.6 illustrates the bandgaps (or the difference in energy between the valence electrons and the next

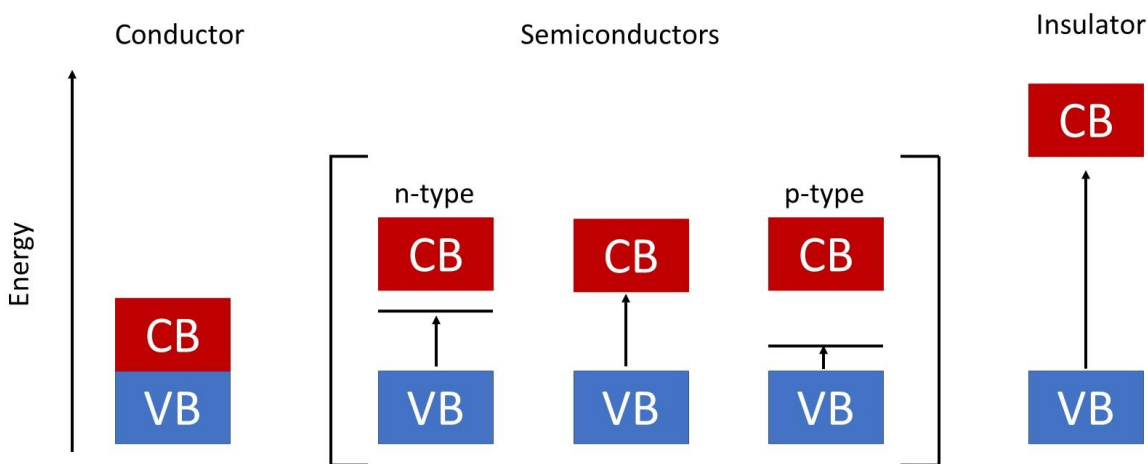


**Figure 1.6.** Energy diagram depicting the relative distance between the valence band (VB) and conduction band (CB) for conductors, semiconductors, including p-type and n-type, and insulators. N-type semiconductors are negatively doped, meaning there is an occupied electronic state within the bandgap such that less energy is needed to excite this electron into the CB. A p-type semiconductor is positively doped, or electron deficient, so the lowest unoccupied energy level is closer to the valence band. See text for discussion of conductors, intrinsic semiconductors, and insulators.



available energy state) of conductors, semiconductors, and insulators. Conductors readily allow the flow of electrons because there is no energetic gap between the valence and conduction bands.<sup>9</sup> Conductors are typically metals such as silver and copper. Semiconductors do have an energy gap between the conduction and valence band, but the magnitude of the gap can be overcome with a relatively small amount of energy. For semiconducting polymers, the structure of the monomer, and how many monomers are present determine the magnitude of the bandgap.<sup>10</sup> Insulators do not conduct electricity due to the large energy gap between the valence band and conduction band. Some common insulators are wood, glass, rubber, or air. Polymers with pi-conjugated systems are interesting and potentially very useful materials because their conductivities range from that of semiconductors ( $10^{-11}$  to  $10^{-3} \text{ Scm}^{-1}$ ) to that of conductors ( $10^{-1}$  to  $10^6 \text{ Scm}^{-1}$ ) depending on the composition of the polymer.<sup>1</sup>

Diversity in conductivity is determined by the structure of the monomer unit such as the backbone composition and the chain structure. Several common semiconducting polymers are shown in Figure 1.4. Polypyrrole has a conductivity of ca.  $7.5 \times 10^3 \text{ Scm}^{-1}$ , polyaniline conductivity ranges from 30 – 200  $\text{Scm}^{-1}$ , and poly(3,4-ethylene dioxathiophene) conductivity ranges from 0.4 – 400  $\text{Scm}^{-1}$ .<sup>11</sup>

Polymer conductivity can be further tuned by oxidizing or reducing portions of the polymer.<sup>12</sup> By definition, reduction occurs when an atom, ion, or molecule gains an electron. The reverse of reduction is oxidation, which occurs when an atom, ion, or molecule loses an electron. When the thiophene polymer, or any semiconducting

polymer, is oxidized it functions as a p-type semiconductor.<sup>12</sup> The oxidation of a thiophene monomer is shown in Figure 1.7.

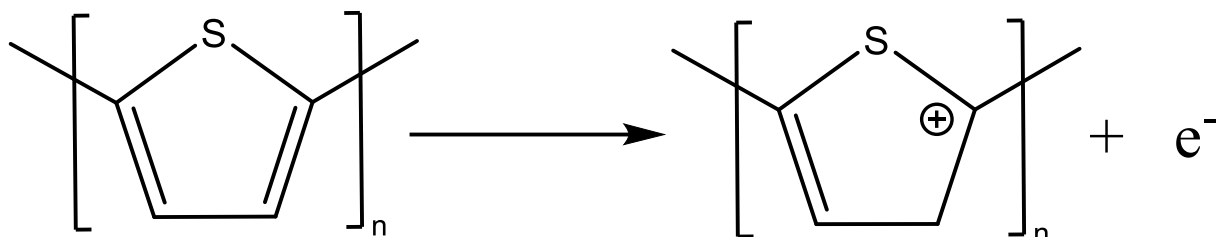


**Figure 1.7.** Oxidation of thiophene monomer, where one electron is removed breaking a carbon-carbon pi bond.

### 1.3 Applications of Conducting Polymers

The diverse properties of conducting polymers allow for a wide range of applications in many fields of science. For instance, biocompatible conducting polymers find utility in many areas of medical technologies such as drug carriers and biosensors.<sup>1,11</sup> The most studied conducting polymers for biomedical devices are polythiophene, polythiophene derivatives, and polyaniline because they are highly biocompatible based on their atomic composition.<sup>11,13</sup> These polymers have been shown to aid in neuro regeneration and drug delivery.<sup>1,14</sup>

Richardson et al. investigated the use of polypyrrole coated electrodes as a method to aid in the preservation of spiral ganglion neurons (SNGs) which causes sensorineural hearing loss.<sup>14</sup> In this study, the polypyrrole coated electrode carried a neurotrophin drug in the cochlea hearing implant, while also providing electrical stimulation that did not damage the implant, demonstrated in Figure 1.8.<sup>14</sup> The hearing implant stored 2 ng of medicine and released a set amount with electrical stimulation into the cochlear, a small

bone inside the inner ear.<sup>14</sup> The study showed that semiconducting polymers that can simultaneously act as a drug-carrier and electrode could be a viable technique in preserving SNGs.<sup>1,11,13</sup>

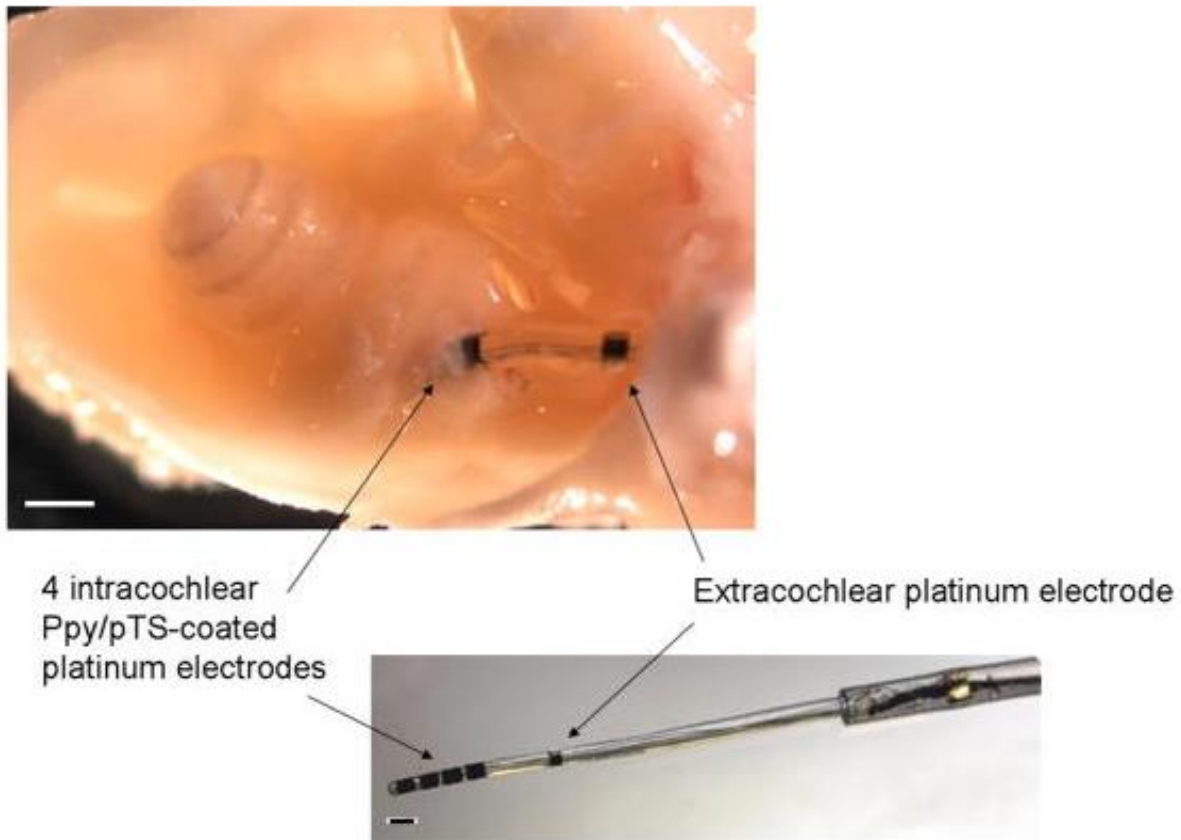


**Figure 1.8.** Polypyrrole coated electrode placed in the cochlear bone in the inner ear. This electrode was used to deliver medicine to this area of the ear to decrease spiral ganglion neurons degradation. This figure is taken from Richardson et al.

Further, the electrical and ionic properties enable the polymers to be used as biosensors or in biocompatible coatings.<sup>1,13</sup> In a study by Pappa et al., a polymer blend containing naphthalene-1,4,5,8-tetracarboxylic diamide unsubstituted bithiophene was used.<sup>15</sup> The polymer was coated with hydrophilic side chains, which allowed the sensor to be injected into the body and transported to a specific area.<sup>15</sup> The purpose of this biosensor was to

detect lactate. When lactate is detected, a change in color occurs on the biosensor indicating that lactate has bonded to an enzyme attached to the sensor, as shown in Figure 1.9.<sup>15</sup> The polymer oxidizes the enzyme-sensor complex and accepts the electron originally from the lactate.<sup>15</sup> The results showed that the semiconductor-based biosensor was more selective, faster, and sensitive than traditional sensors.<sup>15</sup>

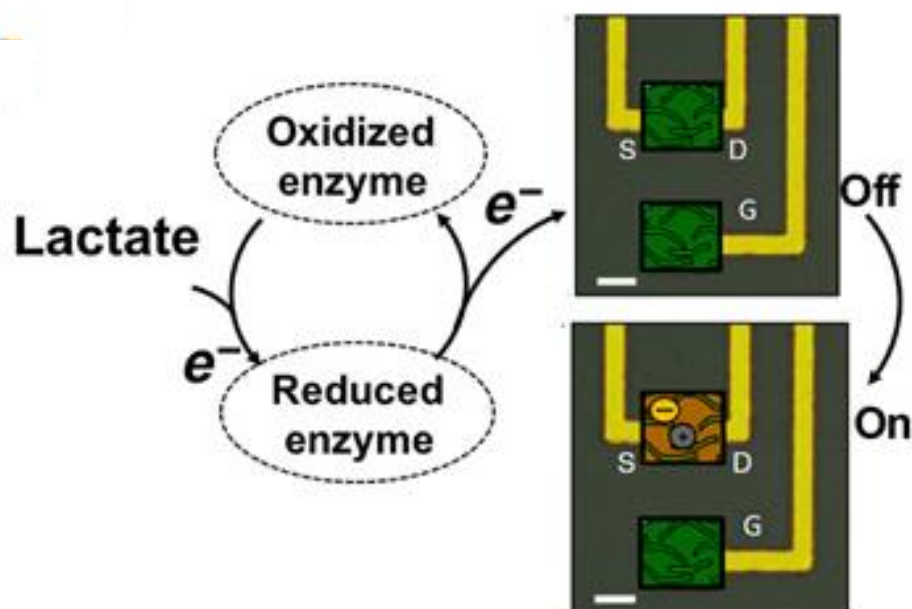


**Figure 1.9.** Diagram of naphthalene-1,4,5,8-tetracarboxylic diimide unsubstituted bithiophene biosensor reacting in the presence of lactate. When lactate and the enzyme on the sensor interact, reduction of the enzyme occurs. When the enzyme is then oxidized on the sensor by the polymer, allowing the electron to be received by the polymer. The orange color change of the S to D sensor indicates that an electron has been accepted, and so alerts the user to the presence of lactate. This figure is taken from Pappa et al.

Polymer based actuators have received great attention because of their potential usage in organic electronics, as well as in biocompatible devices.<sup>16</sup> Actuators are the components of devices that move and control the system in response to some sort of signal or input of energy<sup>16</sup>. An example from work by García-Córdova et al. is shown in

Figure 1.10. In the work done by García-Córdova et al., the three-layered actuator bends in response to net ion movement outside the polymer layers.<sup>17</sup> The actuator movement is a result of it sensing the conditions around, which could be useful for artificial muscles or organs. Other polymer-based actuators bend in response to volume changes within the polymer layers.<sup>1,16,18</sup> A potential is applied the system causing specific ions to flow in or out of the polymer layers.<sup>19</sup> The ion movement results in volume changes within the polymer layer that causes bending.<sup>19</sup> For one polymer layer, an increasingly positive potential would cause cations to enter inducing swelling, and during increasingly negative potentials the polymer would be unaffected.<sup>1,16,18</sup> For the other polymer layer, reduction would cause anions to enter inducing swelling, and during increasingly positive potentials this polymer would be unaffected.<sup>1,16,18</sup> The two different polymer layers provide an actuator that can bend in two different directions due to interactions with differently charged ions.<sup>18</sup>

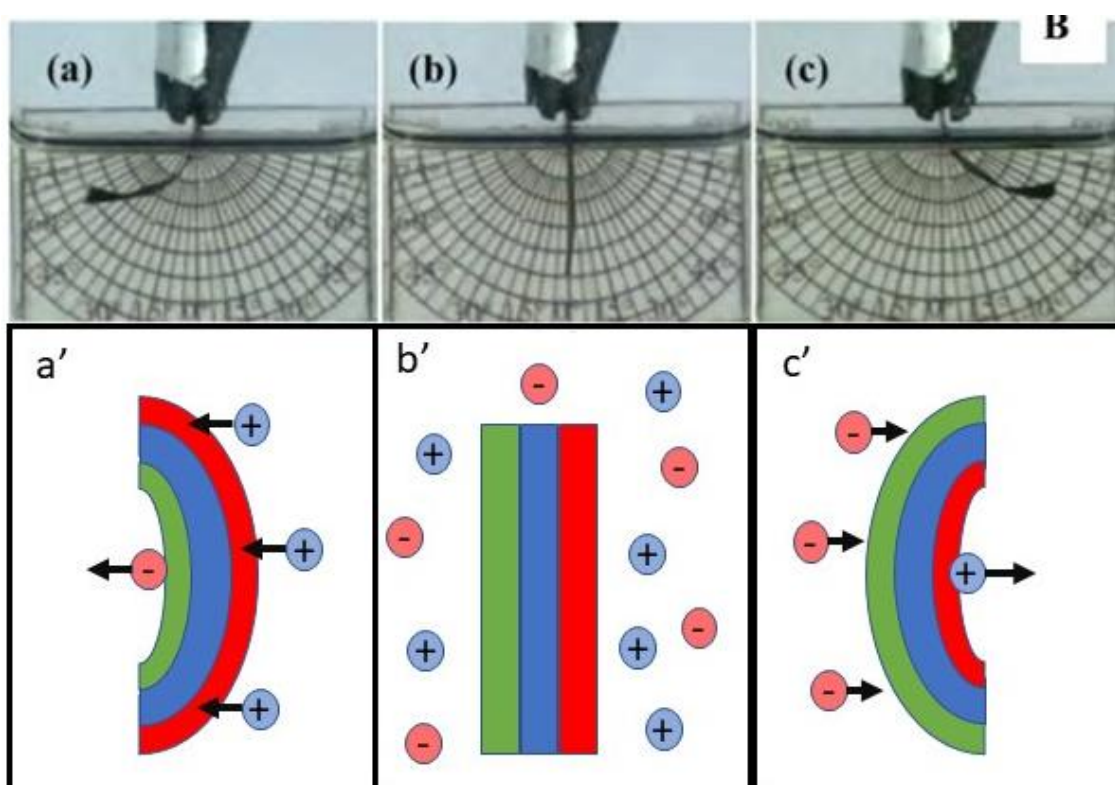


**Figure 1.10.** Polymer based actuator bending in response to current (a, b, c), taken from Ibanez et.al. Cartoon of three-layered polymer actuator bending (a', b', c'). Polymer layers are shown in red and green. Flexible electrode surface is shown in blue. When a potential is applied, ions in solution move into the actuator, causing it to bend in a specific direction.

The polymeric nature of these actuators means that the actuators can be easily tailored to meet the functional needs of the full device. For example, one actuator may need to be thick enough to account for swelling and shrinking of volume or be multilayered to allow for curling and uncurling.<sup>16</sup> One type of polymer-based actuator is artificial muscles; these are typically built from semiconducting polymers and can be classified into two groups: electromechanical and electrochemomechanical.<sup>1,18</sup> The electrochemomechanical actuators respond to changes in current formed from ionic concentrations or applied

potentials, as seen in the work done by García-Córdova et al..<sup>17</sup> Electromechanical actuators function based on changes in faradaic current stimuli.<sup>1,16,18</sup> The physical and electronic processes that enable functionality of polymer actuators will be discussed in detail in Section 1.5 of this introduction.

Electrochromic devices can also be made with conducting polymers.<sup>1</sup> Electrochromic devices have optical properties based on the charge state of the polymer. Structurally, the difference in polymer backbone and chain length give rise to the different observable colors between polymers. Color changes within the same polymer are due to the difference in the electronic structure in the neutral and charged states.<sup>1,12</sup> Electrochromic windows turn dark when a voltage is applied to them and become transparent when the voltage is removed. The voltage, or energy source, for this function can be supplied by solar energy. Different colors can be achieved because the absorption bands change as the polymer is reduced/oxidized. For example, polyaniline changes from an absorption wavelength less than 330 nm to 440 nm when doped.<sup>1</sup> This causes PANI to turn from no visible color at 330 nm, to a dark blue.<sup>1</sup>

Organic electronics, electronics based largely on hydrocarbon systems rather than on traditional inorganic semiconductors and metallic conductors, typically rely on semiconducting polymers. Many organic electronics include multiple semiconducting layers that act as electron donors or electron acceptors.<sup>1,20</sup> Some examples of organic electronics using conducting polymers as the semiconductor include organic light emitting diodes (OLEDs), organic photovoltaics (OPVs), and organic thin-film transistors (OTFTs).<sup>1,20</sup>

Organic light emitting diodes OLEDs consist of many layers, any of which could be composed of small organic molecules or polymers.<sup>1,21</sup> The key active layer of an OLED is the emissive layer, composed of polymer, as the electronic properties of the emissive layer govern the color of light emitted.<sup>1,21</sup> The emissive layer is sandwiched between the electron transport layer and hole transport layer, with electrodes on the outsides of the transport layers as shown in Figure 1.11.<sup>1,21</sup>

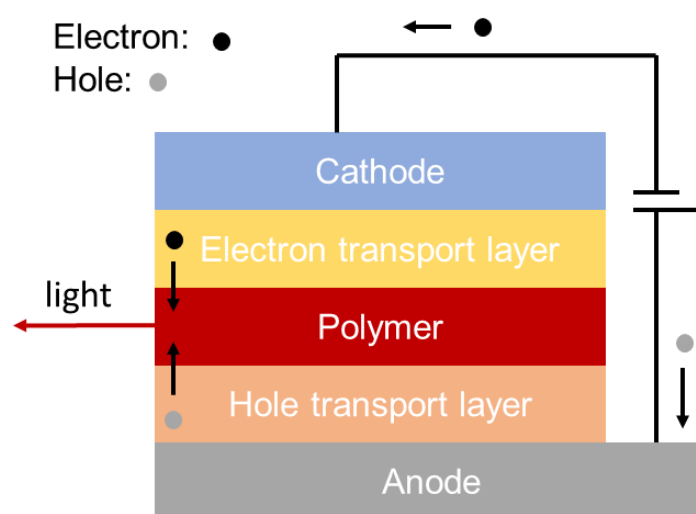


**Figure 1.11.** Structural outline of an organic light emitting diode. Semiconducting polymer acts as the emissive layer, sandwiched between an electron transport and hole transport layer, all between two electrodes. Electrons are introduced into the system from an outside source, electrons travel to the cathode and holes travel to the anode. The electron and hole combine at the emissive polymer layer, and light is generated.

Electrons are introduced at the cathode and flow through the electron transport material.<sup>21</sup> Simultaneously, holes are introduced at the anode and flow through the hole transport layer.<sup>21</sup> The electrons and holes move towards each other and meet at the emissive layer, the electron relaxes down into the hole, and the excess energy is emitted as a photon.<sup>21</sup>



Making the active layers of LEDs from organic materials yields flexible, lighter-weight LEDs, thereby expanding their utility to consumers.<sup>1,21</sup>

The active layers of organic photovoltaics (OPVs), also known as organic solar cells, are composed of organic small molecules or polymers.<sup>1,20,22</sup> The key role of these active layers is to generate power from absorbed sunlight. When light enters the photovoltaic device, an electron in the polymer is excited to a higher energy level, generating both a higher energy electron and a hole, as shown in Figure 1.12. The high energy electron and hole diffuse into the polymer conduction and valence band, respectively.<sup>22,23</sup> Next, the electron relaxes into a lower energy level provided by a second semiconducting polymer.<sup>22,23</sup> Finally, the electron is received at the cathode, and the hole is accepted at the anode where it will be filled with another electron.<sup>22,23</sup> Through this circuit, the energy in sunlight can be used to power other devices or be stored in a battery for later use. As with OLEDs, using polymers to make OPVs can decrease the weight of the OPV and/or increase the flexibility of the resulting devices, both of which are attractive properties for portable electronics.<sup>22,23</sup>

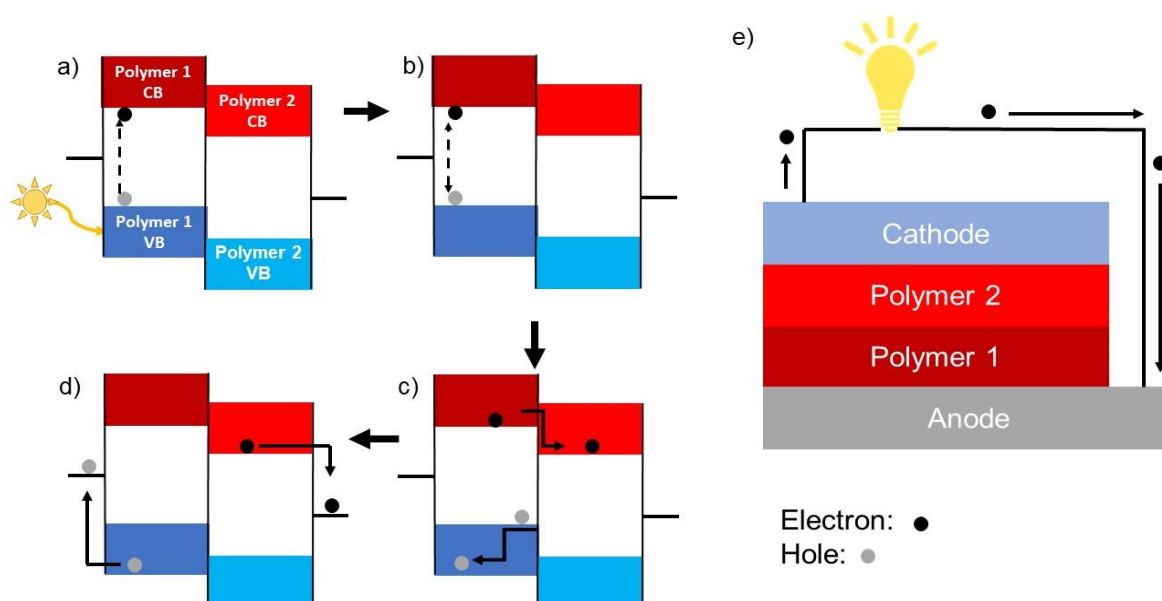


**Figure 1.12.** Structural diagram of an organic photovoltaic cell and electron movement through electrically active layers. First a photon is absorbed in the polymer, an electron is excited to polymer 1's conduction band, and a hole is created (a). Next, the electron and hole diffuse into their respective layers (b). The high energy electron moves through the electron accepting transport layers, polymer 1 conduction band to polymer 2 conduction band (c). The electron is received by the cathode, and the hole is received by the anode (d). Here, a layered structure of an organic photo voltaic cell is shown (e). The electrons generated can be used to power devices or could be stored in a battery for later use.

Despite these and other applications of organic semiconducting polymers, these polymers are limited by their rigidity, instability, and their low solubility.<sup>1</sup> One strategy for improving the functionality of these polymers is blending various polymers or making composites.<sup>1</sup> For example, some semiconducting polymer-based transistors are stable only at ambient temperatures, at higher temperatures, and it would be useful for them to maintain physical stability while at temperatures greater than 150°C.<sup>24</sup> In one study, semiconducting polymers were blended with insulating polymers, where the insulating polymers had a high glass transition temperature.<sup>24</sup> With UV/Vis spectroscopy, they found that heating the nonblended polymer caused the absorption spectra to change, which

was attributed to the polymer changes rearranging with increased temperature.<sup>24</sup> The blended polymer did not give a difference in absorption spectra, implying that there was no rearrangement of polymer.<sup>24</sup> The group also used atomic force microscopy to analyze the morphology of the blended and non-blended polymer.<sup>24</sup> They found similar results of chain rearrangement in the non-blended polymer when heated and no rearrangement in the blended polymer.<sup>24</sup> The introduction of insulating polymer helped the semiconducting polymer maintain structural integrity in high temperatures up to 220°C.<sup>24</sup>

#### 1.4 Polymerization

Another strategy for improving and/or controlling the functionality of semiconducting polymers is by varying the polymerization method. A given polymerization method may be able to impact one or a combination of the following properties: the chain length, the extent of branching and/or crosslinking, and the density. These properties directly impact the electronic properties of the resulting polymers.<sup>1</sup> For instance, a longer chain length (and therefore a longer conjugation length) reduces the energy needed to oxidize the polymer, as the resulting positive charge can be delocalized over more monomer units.<sup>1</sup> More dense and/or more crystalline polymers tend to exhibit higher conductivities, as physical proximity of polymer chains impacts the resistance associated with chain-to-chain electron transfer events.<sup>1</sup>

Two different polymerization techniques are chemical polymerization and electrochemical polymerization. Generally, chemical polymerization involves a chemical reaction to form

a covalent bond between two monomers. For instance, one method of chemical polymerization involves a condensation reaction as shown in Figure 1.13.<sup>11</sup>

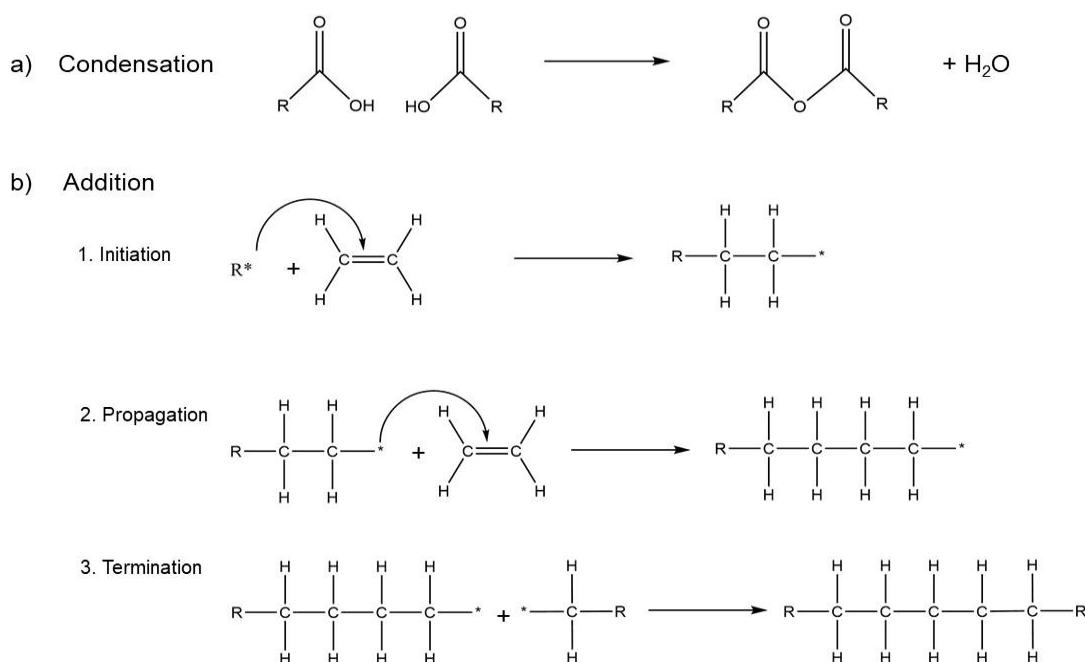


**Figure 1.13.** Single step condensation polymerization, where a bond forms between an oxygen and a carbon, and water is formed (a). Three-step addition polymerization (b) The first step is initiation of a monomer radical, then propagation of the radical polymer, and then termination of the radical polymer resulting in neutral polymer.

In this reaction, a hydrogen from one monomer combines with a hydroxyl group of another monomer.<sup>2</sup> When the bond forms, the hydrogen and hydroxyl group generate water, leaving a covalent bond between the two monomers. Another method of chemical polymerization is through an addition reaction, as shown in Figure 1.13b.<sup>11</sup> Addition polymerization occurs in three steps: initiation, propagation, and termination. A molecule will begin the initiation of polymerization through binding with a monomer. From there, other monomers will lengthen the chain. Eventually, a terminating molecule will cause

termination of the growth. Chemical synthesis offers polymerization processes for a diverse range of polymers, regardless of the electronic properties of the resulting polymers. However, for semiconducting and conducting polymers, electrochemical synthesis is attractive because it eliminates performance-hindering impurities corresponding to chemical oxidizing and/or reducing agents typically used in chemical polymerizations, and it can afford more controlled formation of very thin conducting polymer films.<sup>1</sup> Because electrochemical synthesis, also known as electrochemical polymerization, is used exclusively in the work reported here, the remainder of the introduction will discuss this synthetic method in more detail.

### 1.5 Electropolymerization and Polymer Electrodeposition (Heinze)

Electrochemical polymerization typically occurs in a three-electrode electrochemical cell, where working electrode (WE) is also the substrate upon which the polymer film is deposited.<sup>25</sup> A typical three-electrode cell is shown in Figure 1.14a. In the cell, a solution of electrically neutral monomers, electrolyte, and solvent are present. Electrolyte aids in lowering electrical resistance in the solution.<sup>25</sup> The counter electrode (CE) provides the current necessary to maintain the electrical circuit.<sup>25</sup> The reference electrode (RE) is often composed of a material that has a well-known and understood redox potential.<sup>25</sup>

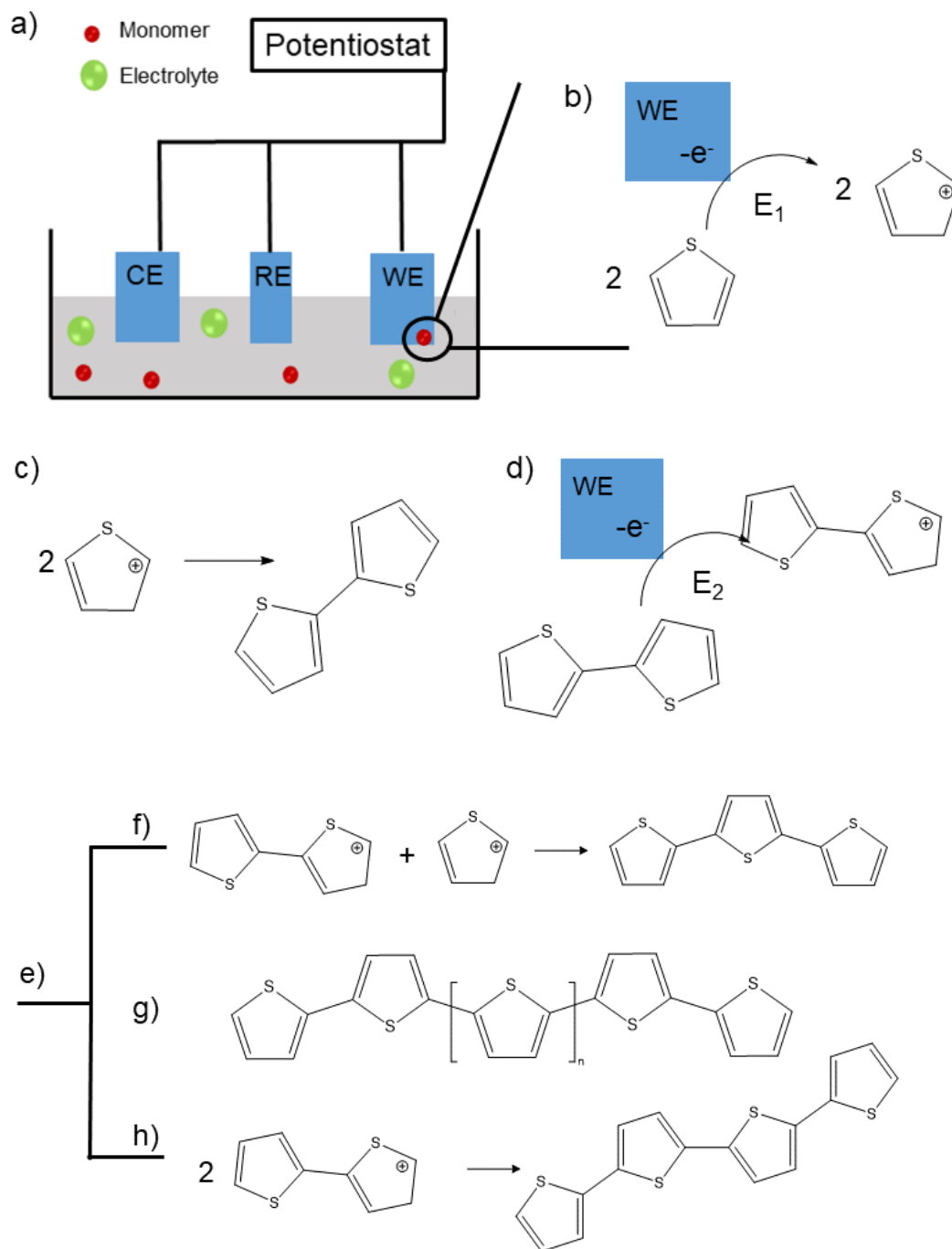


**Figure 1.14.** Electrochemical synthesis of a polythiophene polymer. Three-electrode electrochemical cell includes a solution containing monomer and electrolyte (a). Oxidation of thiophene monomer at the working electrode (WE) (b). Dimerization of two oxidized thiophene monomers (c). Oxidation of dimer at the WE (d). Polymerization pathways (e): dimer bonding with monomer (f), long chain polymer (g), and two dimers combining (h).

In chemical polymerization, a molecular oxidant or reductant generates the charged monomer species that then bond with one another. In electrochemical polymerization, the charged monomers are formed through an electron transfer reaction at the working electrode. In the electrochemical cell, the WE is poised at a potential sufficient for monomer oxidation.<sup>26</sup> As a neutral monomer in solution collides with the working electrode, an electron can be transferred from the monomer to the electrode, resulting in an oxidized monomer very near the electrode surface (Fig 1.14b).<sup>1,26</sup> As additional monomers are oxidized, they can collide with one another to form dimers (two monomer units chemically bound to one another) as shown in Figure 1.14c. Oxidized dimers (Fig 1.14d) can then collide and bond together forming larger oligomers as shown in Figure 1.14e.<sup>26</sup> The energy needed to oxidize a dimer is less than the energy needed to oxidize a monomer, so in Figure 1.14,  $E_1$  is greater than  $E_2$ .<sup>26</sup> When the oligomers contain too many monomer units to remain soluble in the polar solvent, they precipitate onto the working electrode surface in a process termed electrodeposition.<sup>20,26</sup> These surface-bound polymer chains can undergo subsequent oxidations, and oxidized monomers can collide and bond with the polymer chains until the monomer solution near the electrode is depleted, the electrode surface is completely covered with polymer such that no additional monomers can be oxidized, or the electrode potential is changed.<sup>26</sup>

The resulting polymer morphology is difficult to predict and depends on many factors including the structure of the monomer, the deposition time, the deposition rate, and the solubility of oligomers. The structure of the monomer will dictate how close together the monomers and oligomers will bind. The deposition time dictates how thick the polymer

will be. For longer deposition times, the more monomers and oligomers have time to bind, and deposit on to the substrate.<sup>20</sup>

The electronic structure of the electrodeposited polymer is governed primarily by the composition, the polymer chain length, and the polymer microstructure.<sup>1</sup> Additional tuning of the polymer electronic structure can be realized through electrochemical oxidative (or reductive) doping.<sup>12</sup> Electrochemical doping is the process of changing the charge of the polymer through by oxidizing or reducing the polymer charge.<sup>12</sup> Oxidizing a polymer generally converts the polymer to a p-type semiconductor, while reducing the polymer converts the polymer to an n-type semiconductor (see Figure 1.6). To maintain charge neutrality, counterions are physically incorporated into the polymer to offset the charges in the polymer chains.<sup>18</sup>

### 1.6 Electrochemically Stimulated Conformational Relaxation

The electrochemically stimulated conformational relaxation model (ESCR) best describes physical changes, including the reversible volume changes experienced by a polymer, in response to polymer oxidation (or reduction).<sup>18,27</sup> The neutral polymer is compact, as shown in Figure 1.15a. When electrons are removed from the polymer creating areas of positive charge, counter anions are incorporated into the polymer to maintain charge neutrality and the overall volume of the polymer film increases, as shown in Figure 1.15b and 1.15c. At the molecular level, removing an electron from the polymer introduces local flexibility (relaxation) as the pi-conjugation is locally disrupted.<sup>18,28</sup> Diffusion of anions and solvent into the film requires additional rearrangement of the polymer chains, causing the



polymer to swell and increasing the volume of the system.<sup>1,18</sup> As the number of oxidized monomers increases, a corresponding increase in volume is observed. In the reverse direction, reduction of the monomers reintroduces local rigidity, and anions diffuse out of the film while the polymer film condenses to the more compact neutral state.<sup>1,18,27,28</sup>

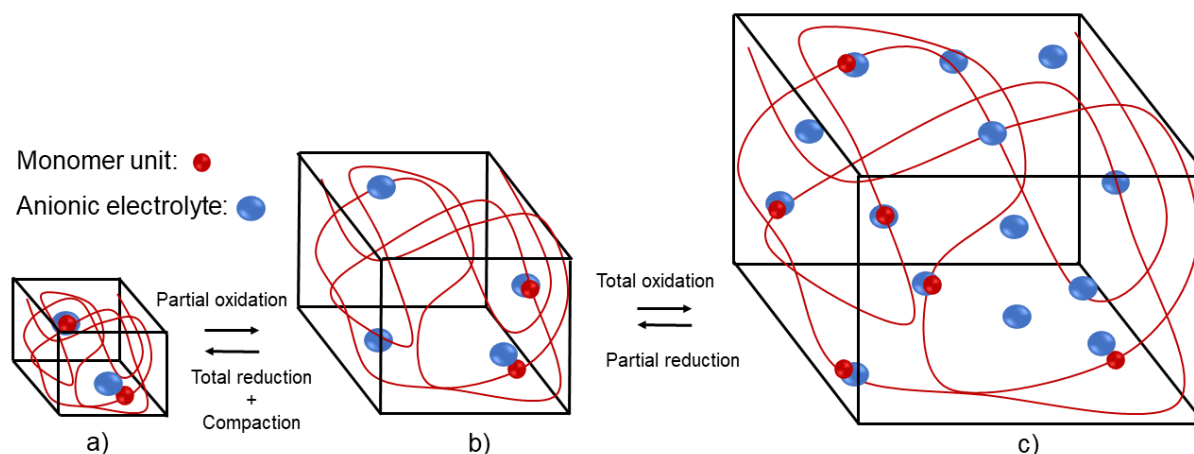


**Figure 1.15.** Electrochemically stimulated conformational relaxation model (ESCR) where neutral monomer is oxidized, and anionic electrolyte causes swelling. The polymer (red) swells as anionic electrolyte (blue) counters positive charge areas created by oxidation. The red-blue interaction illustrates the anionic electrolyte interacting with an oxidized monomer unit on the polymer.

These potential-dependent changes in volume enable the polymer film to function as an actuator, for instance the polymer layer in the actuator will bend as the volume changes which allows it to function like a muscle.<sup>1,19</sup> There can be different types of polymer layers that shrink or swell at different potentials and therefore allow the actuator to bend further or in different directions. The magnitude of change in volume is impacted by polymer microstructure, electrolyte concentration and size, and potential magnitude. Polymer microstructure is influenced by the noncovalent interactions described in Figure 1.2. These interactions influence how much swelling and chain rearrangement can occur to

allow for electrolyte influx. The electrolyte concentration and size influences how many ions are available in solution to flow into the polymer, and to what extent.<sup>27</sup> Higher electrolyte concentrations would increase the amount of swelling because it is more likely for an electrolyte molecule to interact with the polymer. Electrolyte size could impact how well the electrolyte is able to diffuse into the polymer and how well it interacts with a monomer unit.<sup>27</sup> The importance of potential magnitude is evident in Figure 1.15, where the volume increases as the polymer becomes more oxidized due to an increasing potential. As mentioned in Section 1.3, volume changes described by the ESCR model are beneficial to application such as actuators in artificial muscles.<sup>19</sup> However, large volume changes would have adverse effects in other applications such as OLEDs or OPVs. In these devices, the polymer layer is sandwiched between other layers so there is not room for polymer swelling.<sup>21,22</sup> Other applications such as biosensors vary in how much polymer volume is needed for functionality.<sup>13</sup> Understanding how each factor influences polymer swelling is important for developing devices that work efficiently. However, the resulting film morphology and the magnitude of volume change resulting from electrochemically stimulated conformational relaxation is very difficult to predict, motivating the work described here.

## 1.7 Overview

Building upon similar work with poly(3-methylthiophene) and poly(3-hexylthiophene), this work describes the electrochemical polymerization and electrodeposition of poly(3-dodecylthiophene).

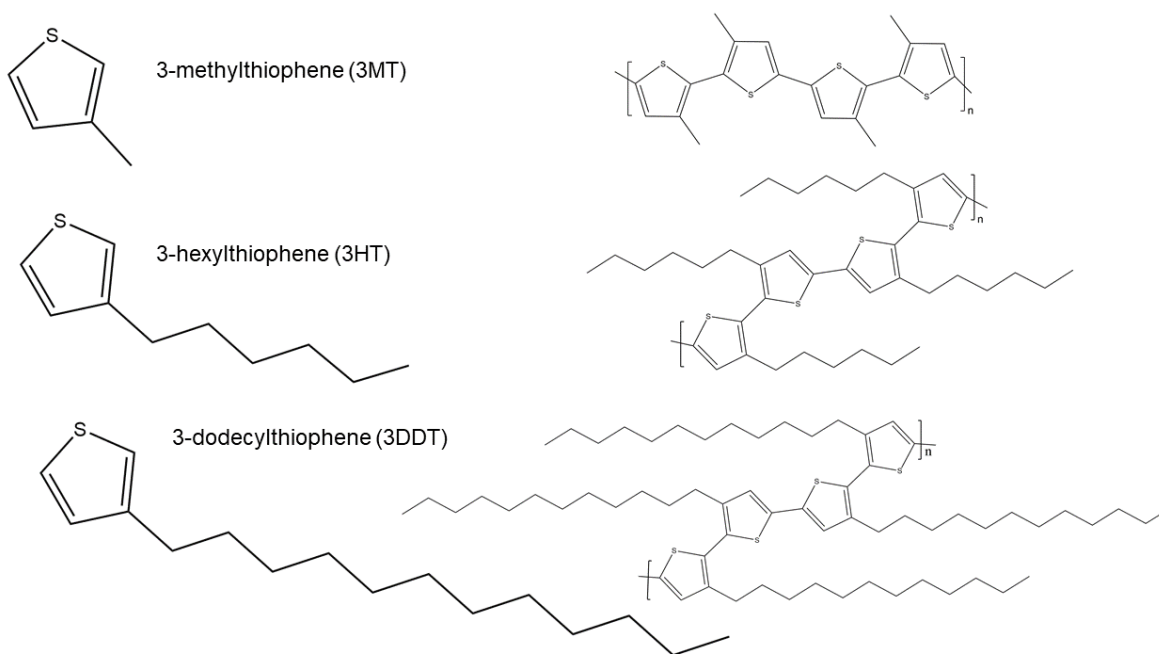


**Figure 1.16** Structure of thiophene derivatives 3-methylthiophene (3MT), 3-hexylthiophene (3HT), and 3-dodecylthiophene (3DDT). Tetramer polymer chain of each monomer with alkyl chain.

We hypothesize that the differences in hydrocarbon chain lengths between these monomers, shown in Figure 1.16, will impact the resulting polymer film morphologies, physical properties such as hardness and compressibility, and the polymer electronic properties.<sup>1</sup> After describing the optimized electrochemical polymerization method, we will discuss the electronic properties of the resulting polymer films as measured by cyclic voltammetry. We will present measured relationships between the amount of charge passed and the polymer film morphology, as measured by atomic force microscopy.

Ultimately, these studies enable determination of relationships between the physical structure of the deposited polymer and the electronic properties of the deposited polymers. Together, this information informs future rational design of organic electronics employing poly(3-dodecylthiophene) as an active layer component.

## Chapter 2: Experimental Methods

### 2.1 Materials and Instrumentation

Acetonitrile (HPLC grade), ethanol (200 proof), tetrabutylammonium hexafluorophosphate (TBAPF<sub>6</sub>, 99.0 %), 57% Hydriodic acid (99.99% trace metals basis), 3-dodecalthiophene (3-DDT), and 3-thiophene acetic acid (3-TAA) were purchased from Sigma Aldrich and used without further purification.

Electropolymerization, electrodeposition, and electrochemical characterizations were performed using a CHI 760E bipotentiostat.

Scanning probe microscopy was performed with an Hitachi 5100n atomic force microscope using self-sensing cantilevers.

### 2.2 Substrate preparation and functionalization

ITO chemical composition, cleaning - Indium tin oxide (~100 nm on glass, sheet resistance ~15 Ω/sq) was purchased from Colorado Concept Coating LLC. Prior to use the ITO substrates were cut into 1-inch squares and cleaned as follows: detergent wash (dilute Triton X-100) and rinse with 18 MΩ water, 15-minute sonication in 18 MΩ water, rinse with absolute ethanol and 15-minute sonication in absolute ethanol. ITO substrates were stored in absolute ethanol until just prior to use.

Functionalization of ITO substrates with surface modifier - ITO substrates were functionalized with 3-TAA using a procedure described by Ratcliff et. al. Briefly, a clean

ITO substrate was covered with hydroiodic acid (57% in water) for 10 seconds, rinsed thoroughly with 18 M $\Omega$  water, and then quickly immersed in 3-TAA (10 mM in ethanol) for a minimum of 12 hours and no more than 48 hours. Just prior to use, a substrate was thoroughly rinsed with ethanol and dried with N<sub>2</sub> (g). The carboxylic acid moiety of the 3-TAA binds indium or tin atoms on the ITO surface, leaving a thiophene free to interact with solution.

### 2.3 Electrochemistry

*Three electrode electrochemical cell:* A 3-electrode electrochemical cell, which consists of a working electrode, counter electrode, and reference electrode, was used for the electrochemical studies described here. The reference electrode was Ag|Ag<sup>+</sup> (10 mM AgNO<sub>3</sub>). The working and counter electrodes were planar indium tin oxide.

*Potential step electropolymerization and electrodeposition:* Electrochemical methods for deposition have primarily used cyclic voltammetry for film growth because it is convenient and easy.<sup>20</sup> However, film properties such as thickness are hard to control when the film is formed with cyclic voltammetry. In this work, potential step electropolymerization was used to better control the rate of film growth and film thickness. P3DDT films were deposited with a potential step using a 50 mmol solution of 3-DDT monomer and of 100 mm TBAPF<sub>6</sub> electrolyte in acetonitrile. Functionalized 3-TAA ITO, as shown in Figure 2.1a, was used as the working electrode with non-functionalized ITO as the counter electrode. The potential was stepped to +1.425 V while the current was measured; the measured current was used to quantify the amount of charge passed. During the potential

step, the 3-TAA was oxidized as were 3-DDT monomers near the electrode as shown in Figure 2.1b.

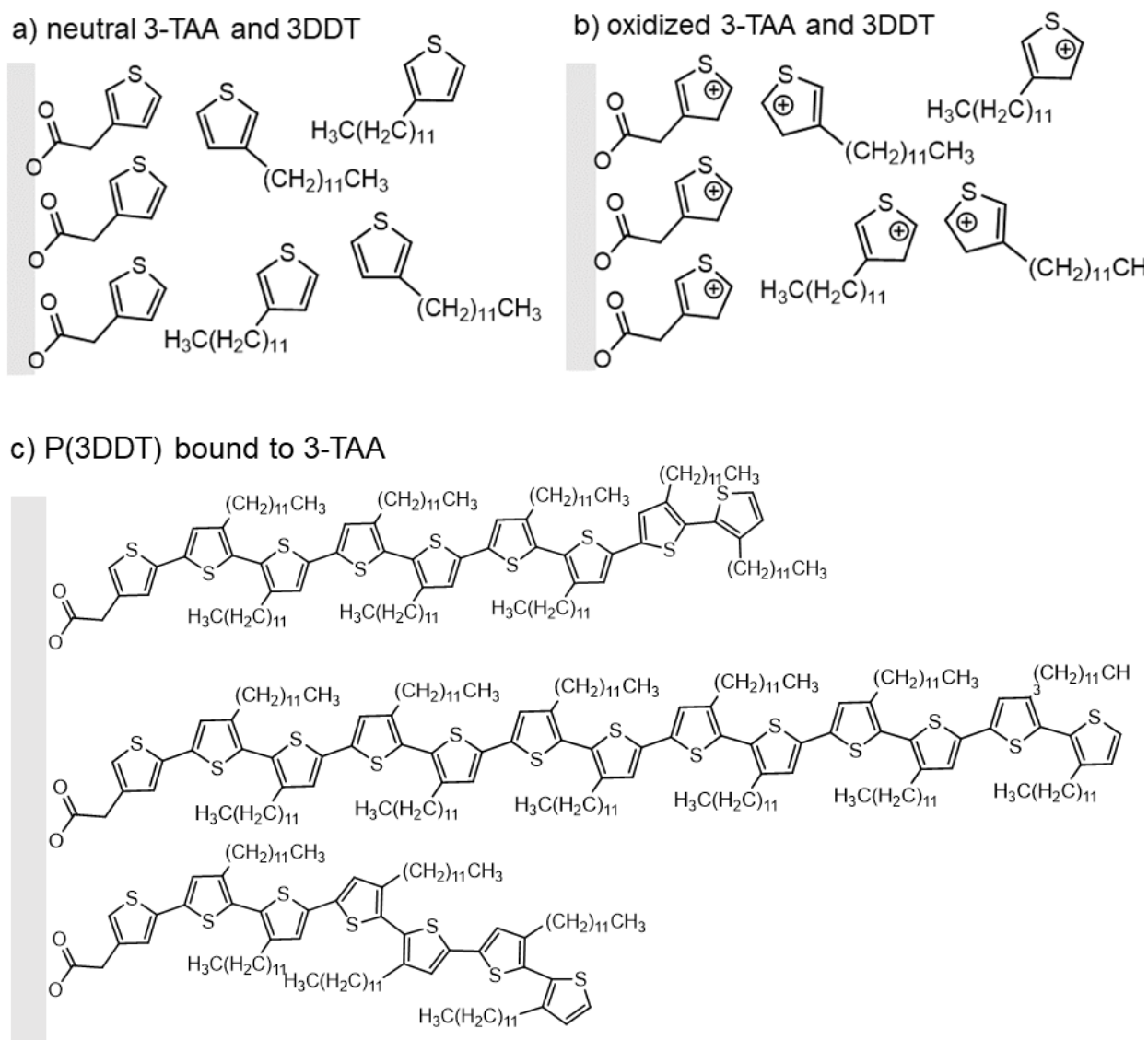


**Figure 2.1** Electrodeposition of 3-DDT onto a functionalized ITO electrode. For convenience the alkyl chain on 3DDT are not fully shown. Neutral monomers and an electrode are in solution (a). A potential is applied such that the monomer and 3-TAA are oxidized. Throughout the potential step, electropolymerization occurs (c), resulting in various chain lengths and directions on the ITO electrode surface.

Oxidized monomers and oxidized oligomers then collide with the oxidized thiophene on the surface such that the resulting polymer film was covalently tethered to the ITO electrode as shown in Figure 2.1c. The amount of charge passed during electropolymerization is proportional to the number of monomers and oligomers that are oxidized. Three different film deposition charges were chosen, and for each Q three films were produced.

*Cyclic voltammetry:* After electrodeposition, the monomer solution was replaced with electrolyte only. Then cell potential was cycled between 0.0 V and +1.1 V at 100 mV/s for 3 cycles. The film was quickly removed, rinsed thoroughly with acetonitrile, blown dry with N<sub>2</sub> gas, and stored in a petri dish for further characterization.

#### 2.4 Scanning Probe Microscopy

Atomic Force Microscopy (AFM) is a type of scanning probe microscopy that is widely used for examining the topography of a material at the nanometer scale. Briefly, the sample is placed onto the scanner, which is then placed directly under the cantilever tip.<sup>29,30</sup> The force-sensing cantilever tip scans the image in the xy plane and records the position changes in the z plane to create a topological image of the material.<sup>30</sup> The scanner will move the sample so that the tip does not move but can still read changes in elevation (Fig 2.2). Elevation differences are initially received in a specific waveform, but a computer converts the data into a line scan that displays height differences.<sup>29,30</sup> Many line traces are collected and put together to provide an overall three-dimensional figure.<sup>29,30</sup> Topography provides information about the surface roughness of the material.



Since the cantilever provides a three-dimensional scan of the material, height information can be determined. Understanding the topography of a material allows one to make assumptions about the formation and stability of it. For polymers, the nucleation process and volume changes according the ESCR model can be observed.

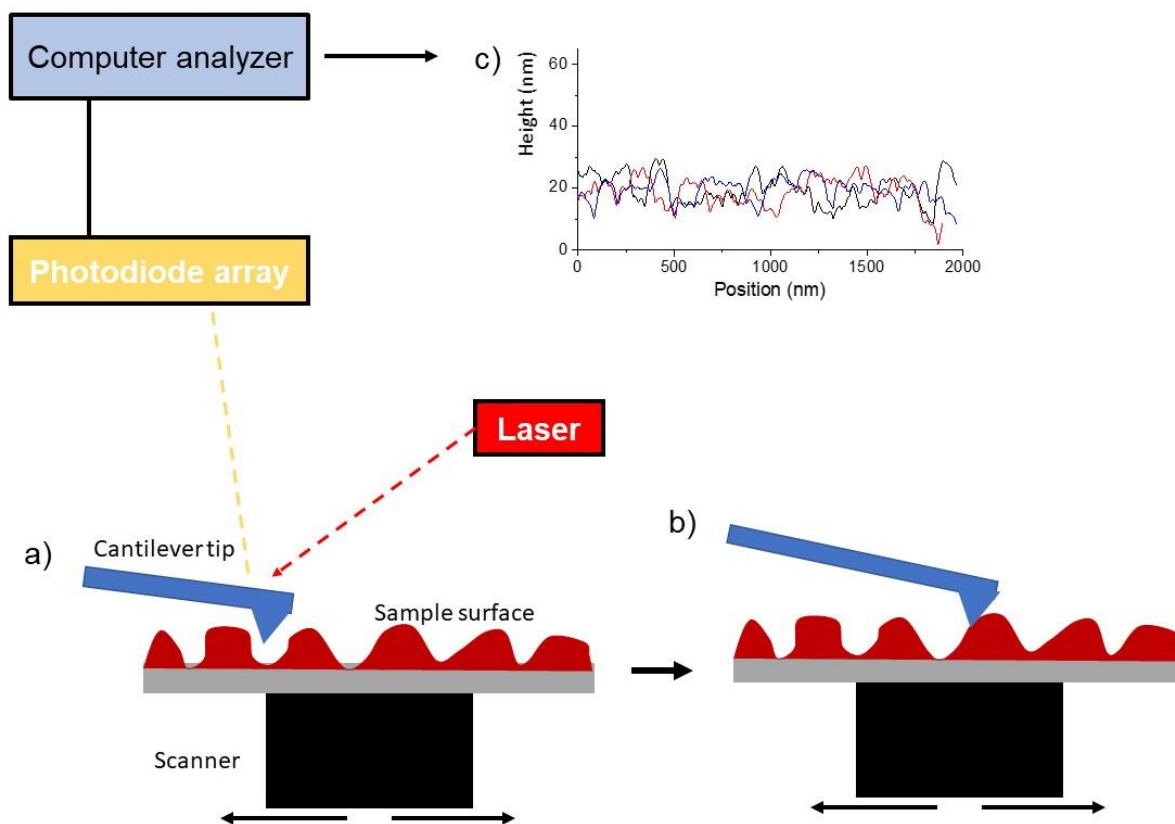


**Figure 2.2.** Atomic force microscope (AFM) diagram. A cantilever tip is rastered across the sample surface moved by the scanner in x and y directions (a). The tip responds to changes in height to perceive the z-axis and the sample is moved by the scanner (b). A laser and photodiode array are used to capture wave functions of the movement. The computer analyzes the data to give us line scans showing height differences on the surface (c).

### **Chapter 3: Electrochemical polymerization, electrodeposition, and characterization of poly(3-dodecylthiophene) (P3DDT) thin films**

Three key questions motivate the work described here. First, we determined the viability of electropolymerization and electrodeposition of P3DDT films from a solution of 3-DDT monomers using a potential step method. Next, we evaluated the relationship between the amount of charge passed during electrodeposition to the polymer film electronic properties with a focus on the measured peak current and integration oxidation wave from cyclic voltammetry of the P3DDT films. Finally, we examined the morphology of the film as a function of charge passed during electrodeposition to glean preliminary information about structure-function relationships.

#### **3.1 P3DDT film electropolymerization and deposition**

The P3DDT films in this work were electropolymerized and electrodeposited from a solution of 3-dodecylthiophene monomers. The potential used (+1.425 V vs Ag|Ag<sup>+</sup> 10 mM) was sufficient to oxidize the 3-thiophene acetic acid on the working electrode (ITO) surface as well as the 3-dodecylthiophene monomers. See Section 2.3 for more details. A representative example of the current generated as a function of time during the potential step is shown in Figure 3.1.

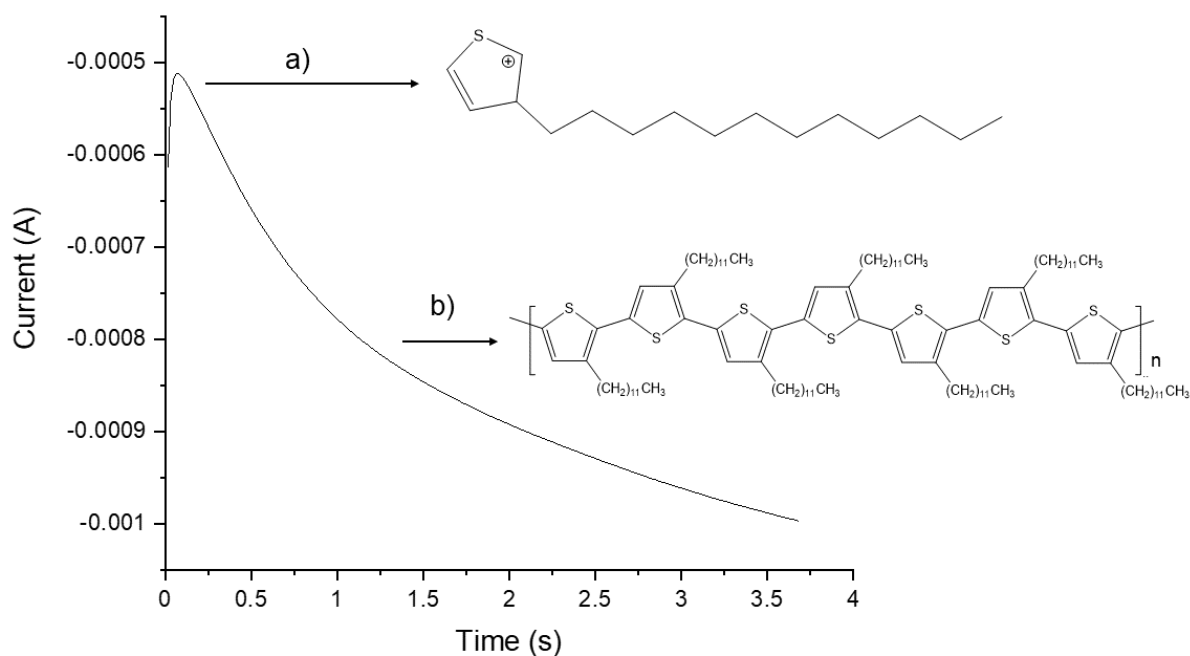


**Figure 3.1** Potential step growth of a representative P3DDT film following a step to +1.425 V. As time increases, additional 3-DDT monomer is oxidized (a). P3DDT polymer begins to deposit onto the electrode surface as time increases and more monomer is oxidized (b).

Non-faradaic processes such as double layer formation were the predominant contributors to the current passed during the first 0.1s, though some of the 3-TAA and 3DDT nearest the working electrode surface may be oxidized during this time as well. At later times, the increasing negative current corresponds to the electrochemical oxidation of 3-DDT monomers and oligomers, which then reacted with one another to form longer oligomers, some of which may be anchored to the ITO surface via a covalent bond between the thiophene moiety of 3-TAA and a P3DDT oligomer (see Fig. 1.14e and Fig. 2.1). Additionally, P3DDT oligomers of sufficient size may precipitate onto the ITO surface. Reactions between the polymer film nucleation sites and oligomers in solution continued until the potential step was stopped. Because the charge passed during the

potential step is proportional to the number of thiophenes oxidized, charge was used to control the amount of P3DDT deposited in each trial. Generally, as the amount of charge passed increases, the amount of P3DDT generated increases as well. Because earlier work with electrodeposited poly(3-hexylthiophene) films correlated increasing charge to increasing polymer film thickness, we hypothesized a similar correlation would be observed with P3DDT films.<sup>20</sup>

### 3.2 P3DDT film electronic properties

Ten P3DDT films were generated, and the electrochemical characteristics of these films are compiled in Table 3.1 including the charge passed during electrodeposition in Coulombs, the peak current ( $i_p$ ) and  $E_{1/2}$  values from a cyclic voltammogram of the film in amps and volts respectively, and integration of the oxidation wave in Coulombs. General trends include correlations between increasing charge and both increasing peak current and increasing charge from the oxidation wave integration, indicating that the amount of polymer electrodeposited does increase with increasing charge.

**Table 3.1.** P3DDT Film Characteristics

<b>Film</b>	<b>Charge (C)</b>	<b>Peak current, <math>i_p</math>, (A)</b>	<b><math>E_{1/2}</math> (V)</b>	<b>Integration of current from CV (C)</b>
1	$-7.97 \times 10^{-4}$	$-1.05 \times 10^{-5}$	0.061	$-5.90 \times 10^{-6}$
2	$-9.19 \times 10^{-4}$	$-1.68 \times 10^{-5}$	0.057	$-1.07 \times 10^{-5}$
3	$-1.24 \times 10^{-3}$	$-2.50 \times 10^{-5}$	0.045	$-1.37 \times 10^{-5}$
4	$-7.40 \times 10^{-4}$	$-1.22 \times 10^{-5}$	0.069	$-7.70 \times 10^{-6}$
5	$-7.76 \times 10^{-4}$	$-1.33 \times 10^{-5}$	0.043	$-8.27 \times 10^{-6}$
6	$-7.56 \times 10^{-4}$	$-1.43 \times 10^{-5}$	0.079	$-8.80 \times 10^{-6}$
7	$-9.03 \times 10^{-4}$	$-1.19 \times 10^{-5}$	0.058	$-6.74 \times 10^{-6}$
8	$-3.12 \times 10^{-3}$	$-6.34 \times 10^{-5}$	0.068	$-3.42 \times 10^{-5}$
9	$-3.09 \times 10^{-3}$	$-6.46 \times 10^{-5}$	0.065	$-3.46 \times 10^{-5}$
10	$-3.10 \times 10^{-3}$	$-6.43 \times 10^{-5}$	0.076	$-3.53 \times 10^{-5}$

To examine these relationships quantitatively,  $i_p$ ,  $E_{1/2}$ , and the integrated charge were plotted as a function of the charge passed during electrodeposition as shown in Figure 3.2.

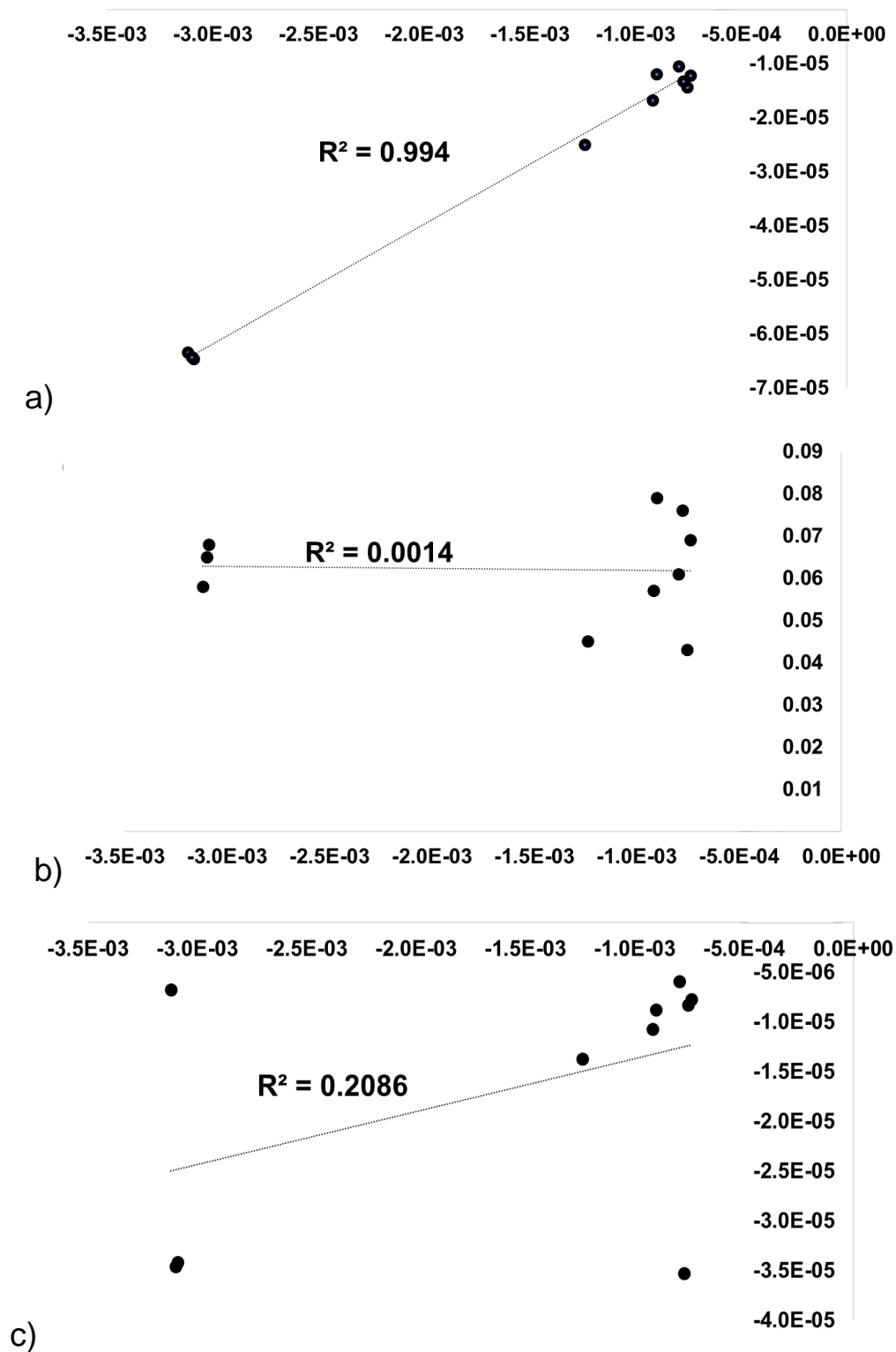


**Figure 3.2** Relationship of charge and  $i_p$  (a), charge and  $E_{1/2}$  (b), and charge and integrated oxidation wave (c).

A linear relationship is seen between charge and  $i_p$ , with a linear fit of 0.994. When charge passed during deposition increased, the peak current of the resulting polymer film also increased. There is no correlation observed between charge and  $E_{1/2}$  values. A small, linear correlation is observed between charge and integrated oxidation wave. Polymer film with more charge allowed to pass during deposition contained more electroactive polymer than film to a lesser charge.

To highlight the differences in P3DDT film characteristics as a function of charge, this section will focus on three representative films, Films 1, 2, and 3.

Cyclic voltammetry was used to characterize the electronic properties of the P3DDT films. The shape of the voltammogram, the peak potentials, and the peak magnitudes are all important parameters to consider when analyzing cyclic voltammograms. The voltammogram shapes result from a combination of factors including concentration of polymer chain length on the electrode, volume changes on polymer film, and changes in film morphology as redox processes occur.<sup>25,28</sup>

When the polymer film is oxidized, Faradaic current corresponding to the electron transfer events can be measured.<sup>25</sup> For every potential at which Faradaic current is observed on the cyclic voltammogram, some portion of the polymer is electrochemically active.<sup>25</sup> Because of the ways the films are made, we expect a dispersion of polymer chain lengths. The broad peaks observed in a cyclic voltammogram of a P3DDT film provide evidence in support of this distribution of chain length, also shown in shown in Figure 2.1c.

Generally, longer polymer chains are easier oxidize because the radical cationic species generated can be delocalized over multiple monomer units.<sup>26</sup> When the potential is swept positively, the current measured from 0.0 V to +0.5 V likely corresponds to oxidation of longer polymer chains. At the peak potential, the most abundant polymer chain lengths are oxidized. As current decreases after the potential, even shorter polymer chains are oxidized. When the potential sweep direction is reversed, beginning at +1.1 V and proceeding towards 0.0 V, the polymer chains are reduced. The shortest polymer chains are reduced first, followed by the reduction of polymer chains of increasing length.

The ESCR model detailed in Section 1.4 describes other processes occurring in the polymer film during oxidation and reduction. Of particular note is the influx of counter anions ( $\text{PF}_6^-$  from the electrolyte) as the polymer is oxidized. The positively charged thiophene rings can persist in the polymer film because positive charges on the polymer are coulombically compensated by these anions. For when the counter anions interact the polymer, the polymer increases in volume to accommodate the influx of ions in the structure (Fig. 1.15).<sup>27</sup> Counter anions are pushed out of the polymer film as the potential becomes is swept in the reduction direction. This causes the volume of the polymer to decrease, and the polymer rearranges to more compact form.<sup>27</sup> The introduction of electrons into the film fills the electron deficient areas on the polymer, making the film neutral again.<sup>27</sup> The anions are not coulombically attracted to the polymer film anymore, and so are repelled.<sup>27</sup>



We also expect a dispersion of microstructure due to noncovalent interactions. For example, electronegative sulfur in the thiophene ring could induce a dipole-dipole interaction between itself and a neutral carbon, described in Figure 1.2. Pi-type interactions are also expected to occur, also described in Figure 1.2. Polymer chains can pile on top of each other, facilitating electrostatic interaction between the pi-bond of one thiophene ring and the electron deficient ring center of a neighboring thiophene ring. These noncovalent interactions also contribute to the broadened peaks observed in Figure 3.4.

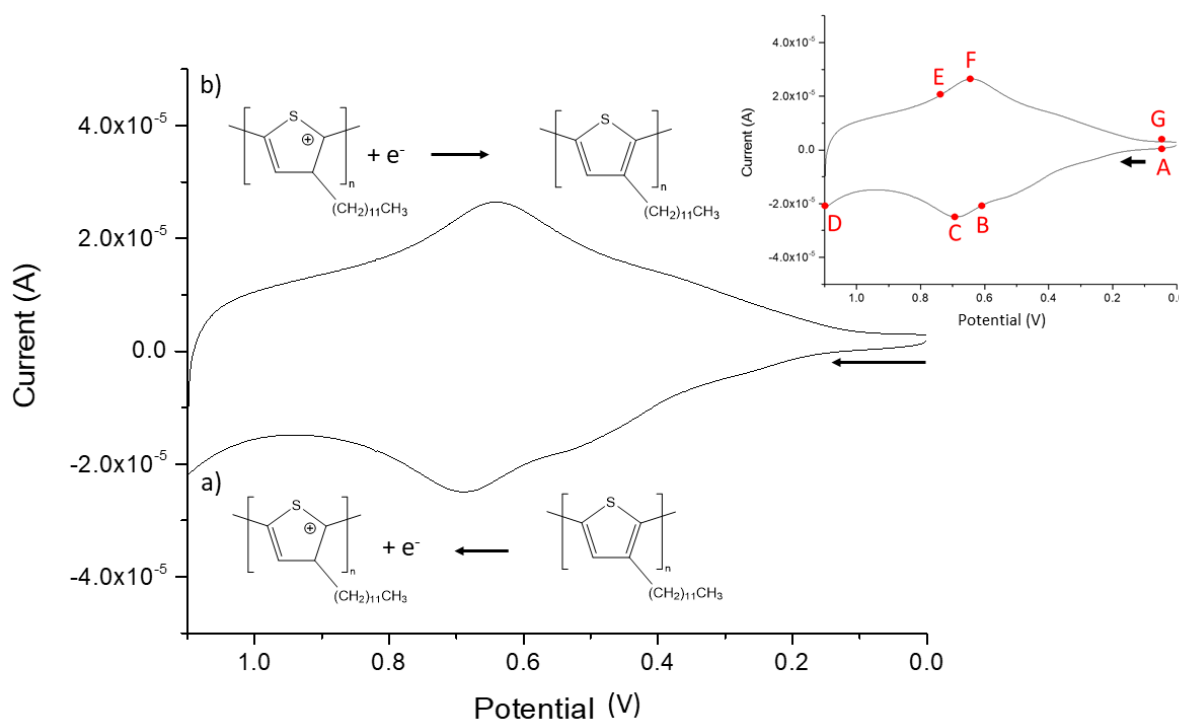


**Figure 3.3.** Cyclic voltammogram of P3DDT illustrating the oxidation (a) and the reduction (b) of the polymer film. Cyclic voltammogram of P3DDT (inset) illustrating the initial potential (A), the oxidative formal potential  $E_{1/2}$  (B), oxidation peak current (C), potential switching (D), reduction formal potential  $E_{1/2}$  (E), reduction peak current (F), and potential end (G).

Cyclic voltammograms for the three representative P3DDT films are shown in Figure 3.4. As the potential was cycled from 0.0 V to +1.1 V, the P3DDT film was oxidized, meaning that electrons are transferred from the polymer to the ITO electrode, as shown in Figure 3.3a. As the potential was swept from +1.1 V to 0.0 V, the polymer was reduced via electron transfer from the ITO electrode to the polymer, as shown in Figure 3.3b.

During the oxidation sweep, moving from point A to point D in Figure 3.3 inset, the polymer film generated a negative current as electrons were generated from the film.<sup>25</sup> At point D, the potential switches to move towards lower potentials. At points B and E, the polymer film reached  $E_{1/2}$ .<sup>25</sup> The  $E_{1/2}$  value is an experimentally determined value that is used to estimate the formal potential.<sup>25</sup> Formal potential is the potential at which oxidized and reduced species are in equilibrium.<sup>25</sup> Point C indicates the oxidation peak, where the current produced is dictated by the oxidation of the most abundant polymer chain lengths.<sup>25</sup> Point F is the reduction peak, which is dictated by the reduction of the most abundant chain lengths. Point D indicates the reduction peak; the reduction of the most abundant polymer chain lengths determines the current produced. The oxidation and reduction peaks provide information on the maximum amount of current that can be produced from the polymer film. In the cyclic voltammograms shown in Figure 3.4, we can see that the area under the oxidation peaks and reduction peaks, points C and F, increased as the charge deposited to increased. We have calculated this value as integrated oxidation wave, which did show a linear correlation with increasing charge during deposition. This information confirms that the amount of electroactive polymer increased with increasing charge during deposition.

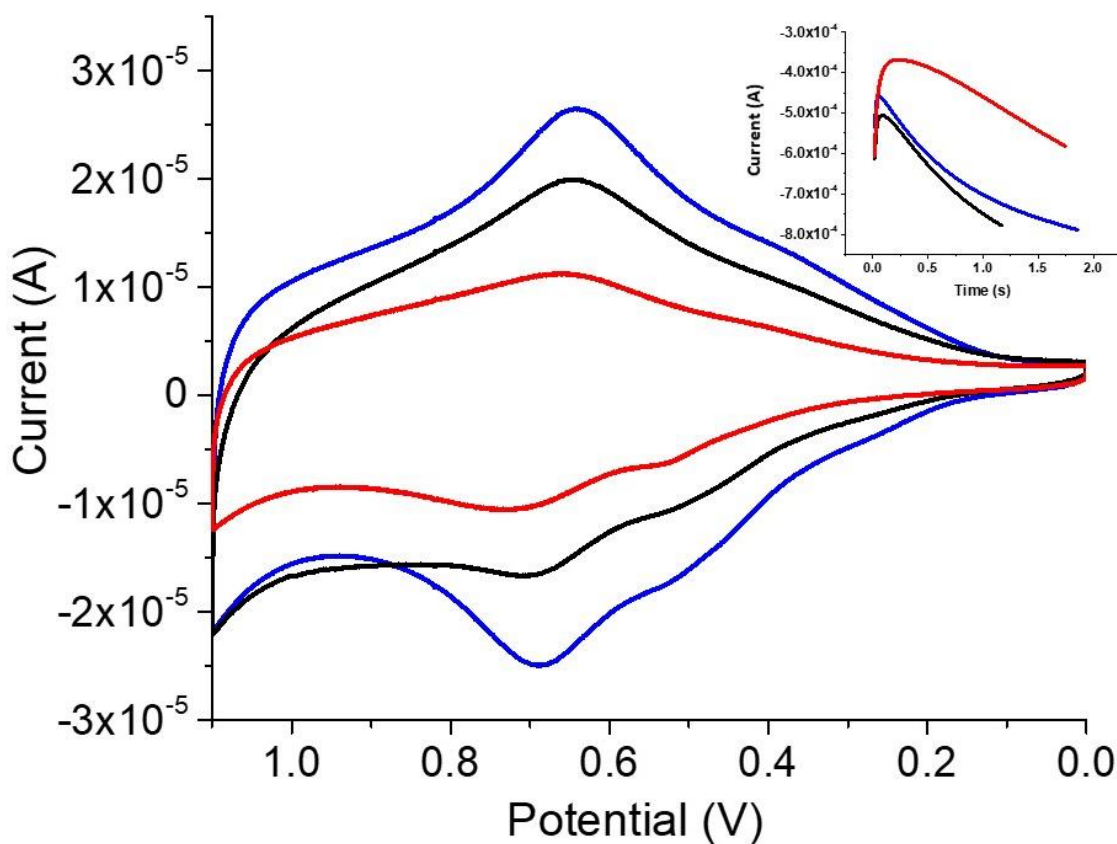


**Figure 3.4.** Cyclic voltammograms of P3DDT films 1 (red), 2 (black), and 3 (blue), with corresponding electrodeposition traces inset. Voltammograms were collected directly following electrodeposition in a solution of 0.1 M TBAPF<sub>6</sub> at 100 mV/s.

The oxidation and reduction peak potentials do not remarkably change as charge passed during electropolymerization increases. Since the composition polymer produced was not chemically changed during any trial, we expected each polymer film to have oxidation and reduction peaks centered near the same potential. For these films, the oxidation potential of the most abundant chain length is ca. +0.7 V. Oxidation of longer polymer chains can be seen as the current increases while potential increase from 0.0 V to +0.6

V for all 3 films. Evidence of longer polymer chains is also observable in the reduction sweep, from +0.6 V to 0.0 V, as the current decreases.

Another noticeable feature in these voltammograms is a disproportionate increase in oxidation current from 0.0 V to +0.4 V as the amount of polymer in the film increases. The disproportionate increase likely results from variations in dispersion interactions. Longer polymer chains are more likely to experience noncovalent interactions because there is more polymer surface area available for interaction with other polymer chains. Therefore, a less positive oxidation potential was needed for longer polymer stabilized by noncovalent interactions, as the cationic species of these chains experience additional stabilization from the neighboring chains.

The oxidation and reduction peak currents increase as charge passed during electropolymerization increases. An increase in peak current can be seen in Figure 3.3, as the peak current for Film 1 is much smaller in magnitude than the peak current in Film 3. The area of the current peaks for Film 1 is smaller than Film 2, and both are smaller than Film 3. While the distribution of chain lengths for the 3 films are similar, the amount of chains at a given length increases as charge measured during electropolymerization increases. Ultimately, the increase in peak current as charge passed increases confirms that the amount of electroactive polymer film linearly increases as the amount of charge passed during electrodeposition increase.

Further, integrating the current during an oxidative sweep quantifies the amount of electroactive polymer on the ITO electrode. The integration of each oxidative sweep increases as charge passed during electropolymerization increases. The linear fit for all 10 films showed a weak, linear relationship between charge and the integration of charge. With consideration of possible outliers due to a margin of error, the linear relationship may have been stronger. During electropolymerization, the current measured likely corresponds to the oxidation of monomers and oligomers. However, not all the oxidized monomers and oligomers will polymerize enough to deposit onto the electrode. Integration of the oxidative sweep for each polymer film provides a more accurate measurement of the amount of polymer that was deposited onto the electrode. The trends shown from peak current integration of the peak provide evidence that the charge measured during electropolymerization does correspond to the amount of polymer film deposited. While both features, peak current and peak current integration show that charge measured corresponds to amount of deposited polymer, there were slight variations in these correlations. For example, while the charge passed for Film 1 was larger than Film 6 ( $-7.9661 \times 10^{-4}$  vs.  $-7.5639 \times 10^{-4}$ ), the peak current in Film 6 was larger ( $-1.054 \times 10^{-5}$  vs.  $-1.432 \times 10^{-5}$ ). The three films chosen to demonstrate the major findings because they communicated the features studied best. However, when considering all 10 films there is a noticeable margin of error.

### 3.3 P3DDT film atomic force microscopy

While electrochemical characterization of the P3DDT films provides valuable information about the amount and electronic properties of P3DDT present in a given P3DDT film, additional characterization is needed to determine the polymer morphology, as the morphology of the resulting polymer film is critically important to its function. Depending on the use of the polymer film, one or a combination of conformal coverage of the electrode, film thickness, and film roughness/surface area may be optimized to yield desirable polymer film characteristics.

Atomic force microscopy topography images of the ITO substrate and of three representative P3DDT films are shown in Figure 3.5. As discussed in Section 2.4, AFM uses a very small probe scanned back and forth across a sample to generate a landscape-like view of the surface at the microscale. In these images, the color gradient

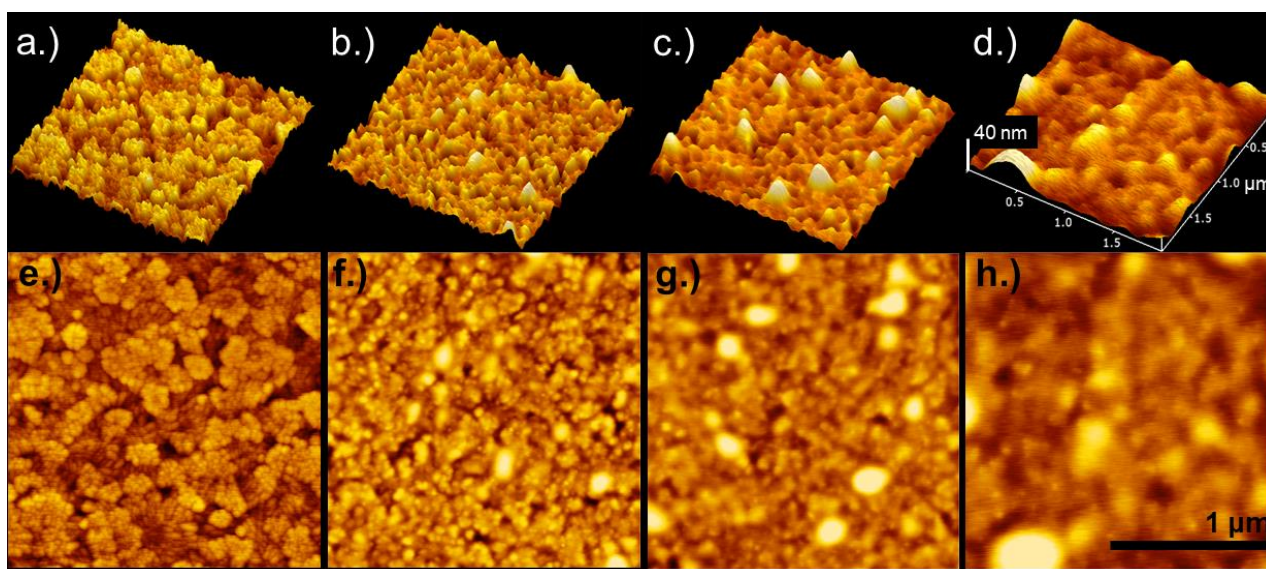


**Figure 3.5.** AFM topography images presented in 3 dimensions (top) and two dimensions (bottom) of ITO (a, e), Film 6 (b, f), Film 2 (c, g), and Film 3 (d, h). All images correspond to a representative  $2\ \mu\text{m} \times 2\ \mu\text{m}$  square of the sample. The dimensions given in (d) and (h) correspond to (a-d) and (e-h) respectively.

indicates the height of a feature, where the lightest colors correspond to the tallest peaks and the darker colors correspond to lowest valleys. In these images, the tallest features peak around 40 nm. Each image corresponds to a 2  $\mu\text{m}$  by 2  $\mu\text{m}$  square of the substrate of film.

The ITO microstructure showing cauliflower-like nodules is distinctive and consisted with literature.<sup>20</sup> Based on similar work with electrodeposited poly(3-hexylthiophene) we hypothesized that all of these polymer films would cover the ITO electrode conformally and would increase in thickness as charge passed during electrodeposition increased.<sup>20</sup> However, parts of the underlying ITO microstructure are clearly evident in Films 1 and 2, indicating that conformal polymer film coverage was not realized in these two films. Additionally, the z-scale for all 3 polymer films is similar, with the highest points reaching 35-40 nm in all films. In Film 6, there is a relatively high density of bright spots distributed relatively evenly across the samples. These tall (bright) spots correspond to polymer film nucleation sites – the places where polymer first started to deposit onto the ITO electrode. In Film 2, there are fewer tall (bright) spots, and the sizes of the spots appears to increase indicating additional polymer deposition around the nucleation sites and the coalescence of some nuclei. In Film 3, a few small tall (bright) spots remain, but larger tall mounds of polymer are evident and features corresponding to the ITO substrate are obscured by the P3DDT film, indicating conformal film coverage is achieved in this film.

The RMS surface roughnesses and the surface areas of the ITO substrate and all P3DDT films examined in this work are given in Table 3.2. Interestingly, both the surface

roughness and surface area decrease slightly when any amount of polymer is deposited onto the ITO substrate. However, no clear correlation between charge passed during electrodeposition (functionally, the amount of polymer on the surface) and either of these two parameters is observed. Together, these AFM data are consistent with a nucleation and three-dimensional growth model for polymer electrodeposition.<sup>1,26</sup>

**Table 3.2.** AFM measurements of RMS surface roughness and surface areas

Film	Charge	RMS Surface Roughness (nm)	Surface Area (nm <sup>2</sup> )
ITO		4.49	5.15 x 10 <sup>6</sup>
1	-7.97 x 10 <sup>-4</sup>	4.20	5.80 x 10 <sup>6</sup>
2	-9.19 x 10 <sup>-4</sup>	4.18	4.15 x 10 <sup>6</sup>
3	-1.24 x 10 <sup>-3</sup>	4.17	4.45 x 10 <sup>6</sup>
4	-7.40 x 10 <sup>-4</sup>	4.62	4.22 x 10 <sup>6</sup>
5	-7.76 x 10 <sup>-4</sup>	3.09	4.24 x 10 <sup>6</sup>
6	-7.56 x 10 <sup>-4</sup>	3.97	4.34 x 10 <sup>6</sup>
7	-9.03 x 10 <sup>-4</sup>	5.75	4.61 x 10 <sup>6</sup>
8	-3.12 x 10 <sup>-3</sup>	14.5	4.10 x 10 <sup>6</sup>
9	-3.09 x 10 <sup>-3</sup>	Unable to measure	Unable to measure
10	-3.10 x 10 <sup>-3</sup>	10.9	4.09 x 10 <sup>6</sup>

We have shown that electropolymerization and electrodeposition of 3-DDT monomer to form P3DDT polymer through a potential step is a viable polymerization technique. The electronic properties of P3DDT polymer films were evaluated, focusing specifically on the



relationship between charged passed during polymerization to the measured peak current and integration oxidation wave from cyclic voltammetry of the P3DDT films. We found that the amount of electroactive polymer increases as charged passed during deposition increased based on linear relationships between charge and both peak current and integration of the oxidation wave. Atomic force microscopy data showed the nucleation and growth of P3DDT films which was consistent with three-dimensional polymer growth. The RMS surface roughnesses and the surface areas showed no correlation to the amount of charged passed during polymerization.

## Chapter 4: Conclusions & Future Directions

From this work, we found that as charge passed during electrodeposition increases, the amount of deposited polymer also increases. Peak current and peak integration data support this through their linear relationship with charge passed during deposition. The electronic properties of the P3DDT films were characterized through analyzing the shape of the cyclic voltammograms. Future analysis of these trends will include a spectroscopic characterization to relate current peaks in a cyclic voltammogram to polymer film optical properties. Additionally, films with more electrodeposited polymer will be examined.

Atomic force microscopy data show the nucleation and subsequent growth of P3DDT. Each polymer film began with individual, discrete nucleation sites that began to coalesce as additional polymer deposited. Future studies will examine whether volume changes predicted by the ESCR model are experienced by P3DDT using AFM as a function of film thickness. We will also determine whether film thickness is controllable with charge once a critical conformal thickness has been reached.

Information gained from these studies will provide necessary understanding for the development of organic electronics utilizing semiconducting polymer. In these electronics, it is important to control film thickness so that the chemical and electrical properties can be tailored to fit the function of the device such as volume changes and producible current.

## References

- (1) Ibanez, J. G.; Rincon, M. E.; Gutierrez-Granados, S.; Chahma, M.; Jaramillo-Quintero, O. A.; Frontana-Uribe, B. A. Conducting Polymers in the Field of Energy, Environmental Remediation, and Chemical-Chiral Sensors. *Am. Chem. Soc.* **2018**, *118*, 4731–4816.
- (2) Loo, J. S. C. From Plastics to Advanced Polymer Implants: The Essentials of Polymer Chemistry. *COSMOS* **2008**, *4*, 1–15.
- (3) Umar, Y. Polymer Basics: Classroom Activities Manipulating Paper Clips To Introduce the Structures and Properties of Polymers. *J Chem Educ* **2014**, *91*, 1667–1670.
- (4) Sterner, E. S. Three Ways to Polyamides: The Impact of Polymerization Mechanism on Polymer Properties. *J Chem Educ* **2019**, *96*, 2003–2008.
- (5) Wheeler, S. E.; Bloom, J. W. G. Toward a More Complete Understanding of Noncovalent Interactions Involving Aromatic Rings. *J Phys Chem A* **2014**, *118*, 6133–6147.
- (6) Knutson, C. M.; Schneiderman, D. K.; Yu, M.; Javner, C. H.; Distefano, M. D.; Wissinger, J. E. Polymeric Medical Sutures: An Exploration of Polymers and Green Chemistry. *Am. Chem. Soc.* **2017**, *94*, 1761–1765.
- (7) Pillai, C. K. S.; Sharma, C. P. Review Paper: Absorbable Polymeric Surgical Sutures: Chemistry, Production, Properties, Biodegradability, and Performance. *J. Biomater. Appl.* **2010**, *25*, 291–366.
- (8) Heeger, A. J. Semiconducting Polymers: The Third Generation. *Chem Soc Rev* **2010**, *39*, 2354–2371.
- (9) Weller, M.; Overton, T.; Rourke, J.; Armstrong, F. *Inorganic Chemistry*, 7th ed.; Oxford University Press: New York, NY.
- (10) Brédas, J.; Marder, S.; Andre, J. *An Introduction to the Electronic Structure of  $\pi$ -Conjugated Molecules and Polymers, and to the Concept of Electronic Bands in the WSPC Reference on Organic Electronics: Organic Semiconductors*; World Scientific Publishing Company: Hackensack, NJ, 2019; Vol. 1.
- (11) Kaur, G.; Adhikari, R.; Cass, P. Electrically Conductive Polymers and Composites for Biomedical Applications. *RSC Adv* **2015**, *5*, 37553–37567.
- (12) Choi, W. T.; Bard, A. J. Doping of the Semiconducting Polymer Poly(3-Hexythiophene) (P3HT) in Organic Photoelectrochemical Cells. *J Phys Chem* **2020**, *124*, 3439–3447.

- (13) Lanzalaco, S.; Molina, B. G. Polymers and Plastics Modified Electrodes for Biosensors: A Review. *Molecules* **2020**, *25*, 1–37.
- (14) Richardson, R. T.; Wise, A. K.; Thompson, B. C.; Flynn, B. O.; Atkinsin, P. J.; Fretwell, N. J.; Fallon, J. B.; Wallace, G. G.; Shepherd, R. K.; Clark, G. M.; O'Leary, S. J. Polypyrrole-Coated Electrodes for the Delivery of Charge and Neurotrophins to Cochlear Neurons. *Biomaterials* **2009**, *30*, 2614–2624.
- (15) Pappa, A. M.; Ohayon, D.; Giovannitti, A.; Maria, I. P.; Savva, A.; Uguz, I.; Rivnay, J.; McColloch, I.; Owens, R. M.; Inal, S. Direct Metabolite Detection with an N-Type Accumulation Mode Organic Electrochemical Transistor. *Sci Adv* **2018**, *4*, eaat0911.
- (16) Lin, H.; Zhang, S.; Xiao, Y.; Zhang, C.; Zhu, J.; J. W. C. Dunliao; Yuan, J. Organic Molecule-Driven Polymeric Actuators. *Macromol Rapid Commun* **2019**, *40*, 1800896.
- (17) Fransisco García-Córdova, F.; Valero, L.; Ismail, Y. A.; Otero, T. F. Biometric Polypyrrole Based All There-In-One Triple Layer Sensing Actuators Exchanging Cations. *J Mater Chem* **2011**, *21*, 17268–17272.
- (18) Keifer, R.; Martinez, J. G.; Keskula, A.; Anbarjafari, G.; Aabloo, A.; Otero, T. F. Polymeric Actuators: Solvents Tune Reaction-Driven Cation to Reaction-Driven Anion Actuation. *Sens. Actuators B Chem.* **2016**, *233*, 328–336.
- (19) Fuchiwaki, M.; Martinez, J. G.; Otero, T. F. Asymmetric Bilayer Muscles: Cooperative Actuation, Dynamic Hysteresis, and Creeping in NaPF<sub>6</sub> Aqueous Solutions. *Chem. Eur.* **2016**, *5*.
- (20) Ratcliff, E. L.; Jenkins, J. L.; Nebesny, K.; Armstrong, N. R. Electrodeposited, “Textured” Poly (3-Hexyl-Thiophene) (e-P3HT) Films for Photovoltaic Applications. *Chem Mater* **2008**, *20*, 5796–5806.
- (21) Gadirov, R. M.; Odod, A. V.; Kurtsevich, A. E.; Ilgach, D. M.; Yakimansky, A. V.; Kopylova, T. N. Multilayer Light-Emitting Diodes Based on Organic Semiconductor Polymers. *Russ. Phys. J.* **2018**, *61*, 1541–1546.
- (22) Akira, T.; Geng, G.; Yanfang, G.; Wei, Q. Tailoring Organic Heterojunction Interfaces in Bilayer Polymer Photovoltaic Devices. *Nat. Mater.* **2011**, *10*, 450–455.
- (23) Shrotriya, V. Organic Photovoltaics: Polymer Power. Nature Photonics. *Nat. Photonics* **2009**, *3*, 447–449.
- (24) Gumyusenge, A.; Tran, D. T.; Lou, X.; Pitch, G. M.; Zhao, Y.; Jenkins, K. A.; Dunn, T. J.; Savoie, B. M.; Mei, J. Semiconducting Polymer Blends That Exhibit Stable Charge Transport at High Temperatures. *Science* **2018**, *362*, 1131–1134.
- (25) Elgrishi, N.; Rountree, J. K.; McCarthy, B. D.; Rountree, E. S.; Eisenhart, T. T. A Practical Beginner's Guide to Cyclic Voltammetry. *J Chem Educ* **2018**, *95*, 197–206.

- (26) Heinze, J.; Rashe, A.; Pagels, M.; Geschke, B. On the Origin of the So-Called Nucleation Loop during Electropolymerization of Conducting Polymers. *J Phys Chem B* **2007**, *111*, 989–997.
- (27) Otero, T. F.; Boyano, I. Comparative Study of Conducting Polymers by the ESCR Model. *J Phys Chem B* **2003**, *107*, 6730–6738.
- (28) Otero, T. F.; Grande, H.; Rodrigues, J. Role of Conformational Relaxation on the Voltammetric Behavior of Polypyrrole: Experiments and Mathematical Model. *J Phys Chem B* **1997**, *101*, 8525–8533.
- (29) Yang, Z.; Craig, D. Q. M. Monitoring Film Coalescence From Aqueous Polymeric Dispersions Using Atomic Force Microscopy: Surface Topographic and Nano-Adhesion Studies. *Asian J. Pharm. Sci.* **2020**, *15*, 104–111.
- (30) Geissibl, F. J. Advances in Atomic Force Microscopy. *Rev. Mod. Phys.* **2003**, No. 75, 949–983.